UNIVERSITY OF CAPE TOWN
IYUNIVESITHI YASEKAPA • UNIVERSITEIT VAN KAAPSTAD

Department of Civil Engineering

Mechanical Behaviour of Steel Hollow Section Columns Subjected to Damage – Experimental Study and Finite Element Modelling

Dissertation submitted in fulfilment of the requirements for the degree of "Master's degree"

Prepared by: Bijal Larknath (LRKBIJ001)

Department of Civil Engineering

University of Cape Town, Private Bag Rondebosch, 7700
South Africa

Plagiarism Declaration

I know the meaning of plagiarism and declare that all the work in the document, save for the properly acknowledged, is my own. This thesis/dissertation has been submitted to the Turnitin module (or equivalent similarity and originality checking software) and I confirm that my supervisor has seen my report, and any concerns revealed by such have been resolved with my supervisor.

Student Number	LRKBIJ001
Name and Surname	Bijal Larknath
Date	23/03/2023
Signature	Signed by candidate

Dedication

This thesis is dedicated to my parents,
Mrs. Catherine Larknath and Mr. Agith Larknath
And my sister, Ms. Kriya Larknath
for their love, encouragement, and support throughout my education.

Acknowledgements

I would like to express my gratitude to God, the Almighty, for His blessings and guidance throughout the progression of this research.

This thesis would not have been possible without the support, assistance, and guidance of several people in the completion of this study.

I am indebted to my supervisor, Dr. Kenny Mudenda, for his invaluable guidance, expertise and feedback which have enabled the progression and completion of this thesis.

To Mr. Thato Miles, the civil engineering laboratory staff and Ms. Penny Louw for their assistance and guidance throughout the experimental testing.

I would also like to extend a sincere thank you to Mr. Greg Mitchell and Mr. Erick Mwang'ingo for their intellectual guidance throughout the finite element modelling process. Your assistance has been invaluable.

Finally, thank you to my friends and colleagues throughout this journey. Your support and encouragement kept me motivated.

This thesis is a success because of the collective efforts of all these individuals throughout this process and I will forever be grateful.

Terms of Reference

This report presents a postgraduate dissertation, conducted in accordance with the requirements of the EMO23CIV01 programme at the University of Cape Town. The topic of this research, which lies in the structural engineering and mechanics field, presents an investigation into the behaviour of steel hollow sections subjected to damage.

The SANS Code 2001-CS1(2005) code states that HSS with damage-induced imperfections need to be replaced, with no tolerances being given to levels of damage that may be acceptable. An investigation was carried out to determine the behaviour of damage on SHS and if acceptable develop a model to retain or repurpose damaged hollow sections. The investigation involved the experimental testing of selected hollow section members. The experimental test results were then used to calibrate/ validate a finite element model. The finite element model was then used to carry out a parametric analysis on the effect of varying levels of damage on member strength.

Table of Contents

List of Figures

List of Tables

List of Equations

Definition of terms and symbols

Technical Terms

Finite Element Analysis	an analysis method whereby a member is separated into a set of parts which are smaller so that an accurate model of the behaviour of the member can be determined using mathematical expressions
Imperfectly sensitive structures	defined as structures with closely spaced eigenvalues.
Youngs modulus	modulus of elasticity
Euler's buckling load	according to Euler's theory the load at which buckling strength of a member happens

Acronyms

BLF	Buckling Load Factor
CIDECT	Comité International pour le Développement et l'Etude de la Construction Tubulaire
ECSA	Engineering Council of South Africa
FEA/M	Finite element analysis/modelling
FLS	Fatigue Limit State
HSS	Hollow Steel Sections
LBA	Linear Buckling analysis
LPF	Load Proportionality Factor
SAISC	South African Steel Construction Handbook
SANS	South African National Standards
SHS	Square Hollow Sections
SLS	Serviceable Limit State
ULS	Ultimate Limit State
UB	Universal Beams

Symbols

A	Member cross-sectional area
Cr	Factored compressive resistance of member of component
E	Modulus of Elasticity
f_u	Ultimate strength
f_y	Yield strength
G	Shear modulus
r	Radius of gyration
λ	Non-dimensional slenderness ratio in column formula
ϕ	Resistance factor for structural steel
λ	Equivalent slenderness

Abstract

Hollow Steel Sections (HSS) are integral components in structural and architectural applications, valued for their torsional resistance, versatility, and aesthetic appeal. These welded steel tubes are typically manufactured off-site and transported to construction sites. However, during transportation, HSS members may incur damage, necessitating replacement in accordance with Sans 2001-CS1 (4.6.1.2) code specifications. This code outlines the criteria and procedures for assessing and replacing damaged HSS members, ensuring adherence to structural safety standards.

This study aimed to assess the behaviour of HSS in response to damage. The objective was to determine the acceptability of commercially available damaged HSS structural specimens. Additionally, it investigated the possibility of retaining and repairing damaged Square Hollow Section members based on the extent of damage.

Experimental testing, complemented by numerical models developed using ABAQUS software for finite element analysis, was employed to achieve these objectives. Various levels of damage were examined using both linear elastic and non-linear buckling analysis approaches. The results indicated a substantial reduction in the failure strength of the HSS members due to damage. However, the elastic buckling loads of the hollow sections were not significantly affected. This observation suggests a certain degree of tolerance in members that may be more prone to elastic buckling failure than material yield failure.

The study acknowledges the potential development of a slenderness ratio specific to the buckling of damaged hollow sections, it ultimately recommends adherence to existing codes governing the repair and replacement of damaged hollow sections as well as provides a decision model based on utilisation of the damaged member. This pragmatic approach emphasises the importance of following established guidelines whilst also taking into consideration tolerances allowed for damaged members, in industry. The decision model provides practical guidance for the assessment and management of damaged HSS members in structural applications. In contrast to the stipulations in SANS Code 2001-CS1(2005), this model provides a selection criterion to either retain the specimen or replace/repair said damaged member.

1. Introduction

1.1 Background to the study

Since the 19th century, Square Hollow Sections (SHS) have been integral to the construction industry, gaining significance with advancements in end preparation and welding technologies. These innovations enabled the fabrication of HSS members into diverse shapes, significantly broadening their applicability in various structural contexts (Wardenier et al., 2010). This investigation aims to thoroughly evaluate the impact of damage on the structural integrity of Square Hollow Section members.

HSS members, known for their adaptability, encompass common cross-sectional shapes such as square, rectangular, and circular configurations, making them essential components in numerous structural applications (Zhao et al., 2005). Their versatility is further accentuated by structural benefits, including superior aesthetic appeal compared to open-section steel members. This aesthetic advantage often positions HSS members as preferred choices in construction applications. The tubular configuration of HSS members contributes to their reliability, exhibiting excellent torsional, compressional, and flexural resistance across all axes (Wardenier et al., 2010).

The hollow design of HSS members not only enhances their structural capabilities but also allows for innovative applications. Incorporating materials like concrete enables the creation of composite sections, showcasing the adaptability and versatility of HSS members in meeting diverse structural requirements. As this investigation unfolds, a comprehensive understanding of the impact of damage on HSS members will contribute valuable insights to their continued effective use in the construction industry.

Square Hollow Section members serve diverse applications, from bridges and airports to warehouses, owing to their adaptability, durability, and dual functionality, seamlessly integrating structural and architectural elements (Lau et al., 2014). However, it is crucial to recognise that the majority of HSS members are manufactured off-site, typically in steel factories. These sections undergo precision cutting, end preparation, and subsequent transportation to construction sites for installation. Throughout this process, spanning manufacturing, transit, and on-site assembly, HSS members are susceptible to damage due to their relatively thin walls.

Localised imperfections, including dents, nicks, and gouges, pose a heightened risk of structural failure to HSS members (Elias, 2020). The presence of these forms of damage significantly influences the structural capacity of HSS members, directly impacting their load-bearing capabilities (Šmak & Straka, 2012). This susceptibility to damage highlights the importance of careful handling and quality control measures during the manufacturing, transportation, and installation phases to mitigate the risk of structural compromise in HSS members.

The fabrication and utilisation of structural steel sections adhere to the guidelines outlined in SANS2001-CS1(2005). This code mandates that all damaged steel components undergo careful

handling to minimise damage and must either be restored to their original fabrication standards or replaced in accordance with the stipulations of the code. However, a limitation of the code is its lack of provision for justifying the replacement of members or offering guidance on evaluating the structural significance of damage suffered by a member that may not significantly affect their load-bearing capacity. This omission has consequences, as the replacement of damaged Square Hollow Section members results in increased costs and material wastage. Addressing this gap in the code is essential for optimising decision-making processes related to the management of damaged structural steel sections.

Several research studies have explored the effects of different load applications on localised imperfections in SHS. Among these investigations are studies focused on cylindrical HSS with cut-outs, such as those conducted by Shariati & Rokhi (2010) and Iman et al. (2018). In one of these studies, finite element analysis was employed, successfully predicting failure loads in tension. However, challenges were encountered in accurately determining buckling loads in compression, where damaged members exhibited buckling behaviours like their undamaged counterparts (Elias, 2020).

It is important to highlight that this study was confined to linear analysis and did not consider non-linear methods for assessing the behaviour of HSS. This limitation emphasises the need for comprehensive investigations that incorporate both linear and non-linear analyses to accurately capture the complex responses of damaged HSS members under different loading conditions.

Further research in this direction would contribute to a more thorough understanding of the structural implications of damage in HSS.

In another study focusing on the effects of dents on hollow sections, it was found that when Square Hollow Section members experience damage, the presence of dents induces material non-linearity due to plastic deformation (Petrusma et al., 2021). This discovery highlights the significance of material behaviour in the presence of damage-induced imperfections.

As a result, a comprehensive investigation into the effects of such imperfections on standard commercial HSS becomes imperative. To ensure accurate evaluation, this research should incorporate both experimental testing and the application of both linear and non-linear analysis methods. By combining these approaches, researchers can obtain a more comprehensive understanding of how damage, particularly in the form of dents, affects the structural response and integrity of SHS members under various loading conditions. This holistic approach contributes to a more comprehensive and accurate assessment of the impact of damage and damage-induced imperfections on the performance of SHS in practical applications.

1.2 Problem definition

The understanding of the effects of damage and damage-induced imperfections on the structural behaviour and risk of failure in SHS remains incomplete. SANS Code 2001- CS1(2005), which governs the fabrication and use of HSS, provides tolerances for physical properties such as size,

thickness, and straightness. However, the standard currently lacks limits for the amounts or areas of damage or damage-induced imperfections that can be tolerated without increasing the likelihood of failure.

According to SANS 2001-CS1 (clause 4.6.1.2), the prevailing practice mandates the replacement of all damaged steel members to adhere to the same physical tolerances as original cast members. Damaged HSS are often sent back to the factory for replacement without a clear understanding of whether the damage has significantly impacted the load-carrying capacity of the member. This approach may lead to increased costs and material wastage, particularly concerning HSS, which are prone to damage due to their thin walls and have higher manufacturing costs compared to other sections (Wardenier et al., 2010).

The current practice of replacing or sending back damaged HSS members to comply with fabrication standards may not be rational if the strength is not significantly impaired. To address this, a thorough investigation is needed. Both linear and non-linear methods of analysis are crucial to accurately predict the buckling behaviour of SHS, considering their geometric and material non-linearities.

This study aims to explore how damage affects the structural strength of standard commercial SHS members, utilising finite element analysis. By employing advanced analytical methods, the research seeks to provide insights into the rationality of existing practices and optimise decision-making regarding the replacement or retention of damaged SHS members in accordance with fabrication standards.

1.3 Objectives

This study aimed to accomplish the following objectives:

- Assessment of strength loss due to varying levels of increasing damage: the primary objective is to assess the impact of varying levels of damage on the structural performance of SHS. This assessment involves quantifying the changes in failure load attributable to these defects.
- Development of a decision model: a critical secondary goal is to formulate a comprehensive decision model for handling damaged members. This model seeks to provide a systematic framework for determining the appropriate course of action when confronted with SHS members exhibiting damage or damage-induced imperfections.

1.4 Scope and Limitations

This investigation analysed the effects of damage or damage-induced imperfections on SHS and subjected to the following limitations:

- Focused Investigation: This research is focused on examining the effects of damage on the load-carrying capacity of Steel Hollow Sections
- Sole Focus on SHS: The scope of this investigation is limited to SHS exclusively, offering

an in-depth exploration of this structural element.

- Combined Approach: To achieve its objectives, this study combines laboratory experiments with advanced modelling software such as ABAQUS for Finite Element Modelling (FEM), enabling a comprehensive analysis of SHS behaviour.

- Exclusive Focus on Damage: The core focus of this research centres on understanding the implications of damage in the form of dents that are modelled as holes, solely within the context of SHS members.
- Based on assumptions that dent material can be represented by an equivalent hole, models considered in this study use holes to represent damage (focus on Part II).

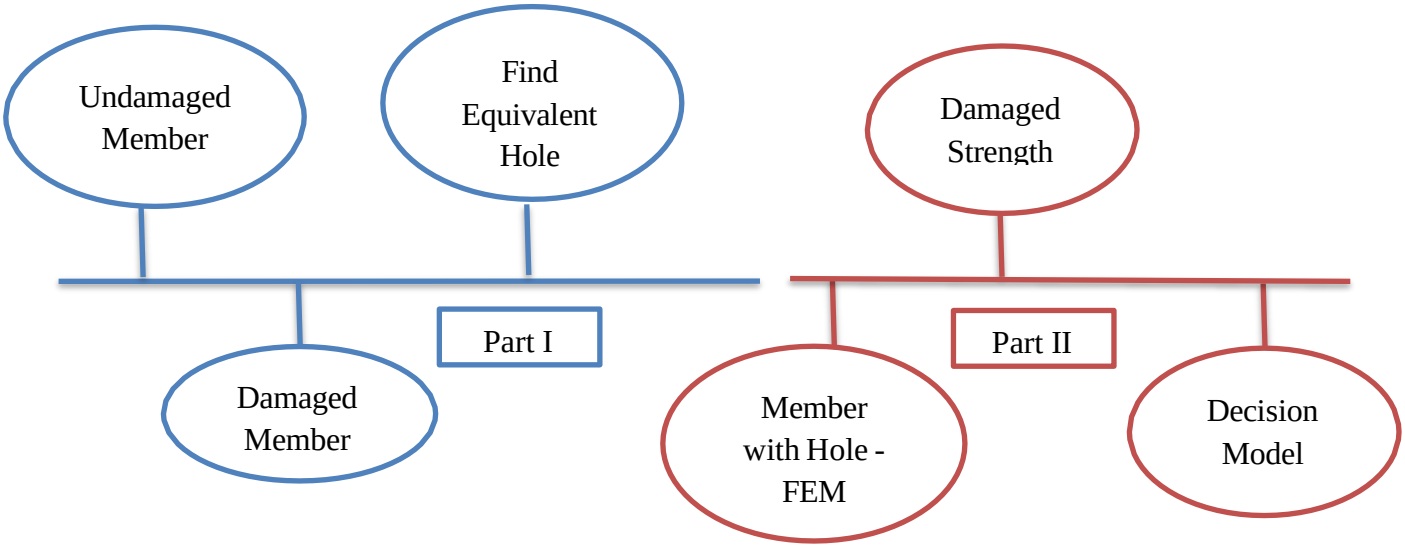

Figure 1-1 Research focus (Part II)

1.5 Report structure

The thesis commences with a succinct introduction, providing a contextual framework for the subsequent literature review. This review constitutes a thorough exploration of relevant literature, encompassing diverse aspects of Square Hollow Section members. It explores the details of SHS member fabrication, delving into their inherent characteristics, and discusses the complex procedures involved in their creation and installation.

Moreover, the literature review systematically scrutinises the susceptibility of SHS members to damage, surveys various methods employed for repairing such damage, and synthesises the findings of prior studies dedicated to understanding the repercussions of damage on the structural performance of SHS members. The literature review looks at the state of knowledge in area of study to reveal gaps in the knowledge.

Following the literature review, the report comprises of the research methodology deployed in this

study, laying the foundation for the investigation's outcomes.

Upon a comprehensive examination of the study's findings, the report provides well-supported conclusions, synthesising the research outcomes and exploring their implications.

In conclusion, the report closes with recommendations for further research, identifying areas where additional exploration could yield valuable insights into this domain.

2. Literature Review

2.1 Steel Hollow Section overview

2.1.1 Description of Steel Hollow Sections

Square Hollow Section members are characterised by a unique design featuring an interior void enclosed by a thin steel wall, giving them their distinctive tube-like shape. Dating back to the 19th century, these tube-shaped specimens have been utilised in notable structures such as bridges, attesting to their exceptional qualities (Wardenier et al., 2010). Their tubular configuration imparts exceptional structural integrity, allowing them to withstand compression, torsion, and flexure in multiple directions (Wardenier et al., 2010). This inherent versatility makes them well-suited for diverse loading conditions (Lau et al., 2014). However, historical limitations in appropriate end preparation methods, design methodologies, and joint construction guidelines had constrained their use in structural applications (Wardenier et al., 2010).

Advancements in end preparation techniques and comprehensive studies on various hollow section joint constructions have gradually overcome these limitations over time. As a result, hollow sections have gained prominence in both structural and architectural applications. With the removal of significant obstacles, extensive research efforts have been directed towards a deeper understanding of hollow section behaviour (Ibrahim & Khalaf, 2018).

In the realm of hollow sections, SHS are often considered a sub-category of Rectangular Hollow Sections (RHS), while Circular Hollow Sections (CHS) are typically produced as standalone entities (Mudenda, 2008). Figure 2-1 provides visual representations of typical hollow section members. Although this study focuses specifically on Square Hollow Section members, a range of other hollow section shapes, including triangular, hexagonal, and octagonal, can also be manufactured (Wardenier, 2001).

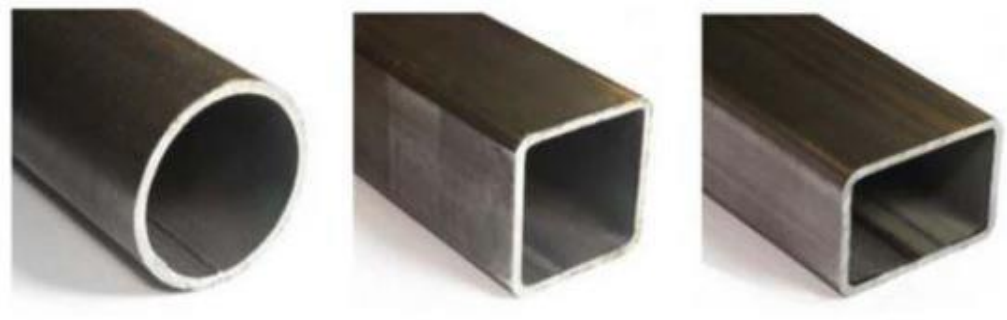

Figure 2-1 Typical Hollow Sections (Narendra & Singh, 2016)

2.1.2 Application of hollow sections

Hollow sections, distinguished by their diverse geometric configurations, serve a myriad of functions and applications in both structural and architectural engineering. These sections are commonly employed in various structural systems, including trusses and lattice frameworks for bridges. Additionally, they play a crucial role in the architectural domain, contributing significantly to the construction of venues such as stadiums and ballrooms. SHS, with their distinctive characteristics, extend their utility to specialised structures like greenhouses and roller coasters. Moreover, they are integral components in offshore installations, masts, power transmission towers, and contribute significantly to building and bridge frames (Wardenier, 2001).

The versatility of hollow sections, particularly their capacity to seamlessly integrate structural and aesthetic considerations, highlights their extensive use in both structural and architectural contexts. These adaptable elements play a vital role in an array of structures, ranging from bridges and roof trusses to steel frames for buildings, wind turbine towers, and even temporary structures like scaffolding. The ability of hollow sections to fulfil diverse roles highlights their importance in enhancing the efficiency and aesthetics of a wide range of engineering and architectural applications.

2.1.2.1 Advantages of hollow sections

- Enhanced Aesthetic Appeal: HSS members offer superior visual aesthetics, making them a preferred choice in architectural and structural applications.
- Multi-Directional Structural Resilience: HSS members exhibit remarkable resistance to torsion, compression, and bending in all directions, enhancing their versatility in various load-bearing scenarios.
- Increased Buckling Resistance: Their tubular design provides greater resistance to buckling, contributing to their structural stability.
- High Strength-to-Weight Ratio: HSS members combine high structural strength with low weight, making them efficient and cost-effective solutions.
- Reduced Corrosion Risk: Compared to other structural steel sections, HSS members are less susceptible to corrosion, extending their lifespan and durability.
- Improved Sectional Resistance: The presence of an internal void enhances their sectional resistance, further reinforcing their load-bearing capacity.

2.1.2.2 History of hollow sections

SHS have experienced a recent surge in utilisation, both in fabrication and structural application, although this adoption has not always been the prevailing practice (Mordini, 2014). The foundational manufacturing methods for creating HSS were established as early as 1886 (Wardenier, 2001). Despite these early developments, connecting HSS members presented significant challenges that impeded their widespread use (Harper, 1976). In the initial stages, connections predominantly relied on methods such as bolting or riveting, predating the widespread adoption of welding during the early 20th century. The geometric intricacies of HSS, especially

CHS, rendered these connection methods unsuitable (Wardenier, 2001). Additionally, the unique design of HSS members made the preparation of their ends for connection a complex and costly endeavour.

While design guidelines have provided validity ranges, there are still areas outside these parameters where the behaviour and strength of joints in HSS components, particularly welded joints, require further understanding (Wardenier, 2001). The mid-20th century witnessed the advent of welding techniques and refinements in fabrication processes, effectively resolving the initial challenges (Wardenier, 2001). The tertiary challenge was addressed in the 1950s, thanks to extensive research efforts, many of which received endorsement from CIDECT. The debate surrounding the utilisation of HSS members persisted until the 1950s when it was finally resolved. However, the widespread adoption of HSS members occurred later than other steel profiles like Universal Beams (UB), which had been in common use since the early 20th century (The Heritage Portal, 2016).

Even today, HSS remains a subject of intensive study in structural engineering (CIDECT, n.d.). Design guides and connection methodologies have evolved through previous research endeavours focusing on HSS members, primarily due to the fabrication, transportation, and erection challenges they presented and continue to pose.

2.1.3 Manufacturing of hollow sections

SHS can be manufactured through three distinct methods: hot forming, hot finishing, and cold forming (Zhang et al., 2016). The selection of the manufacturing method significantly influences the properties of the resulting SHS members, necessitating a comprehensive understanding of the manufacturing processes and their distinctions (Zhang et al., 2016). Furthermore, different design and manufacturing standards apply depending on the chosen method.

In the hot forming process, steel is heated to temperatures, typically around 1200 ºC, and shaped into the desired cross-sectional configuration through rolling or similar techniques. This method produces seamless cross sections without welds (Wardenier, 2001). Conversely, the cold forming process involves bending the steel sheet to the desired shape at ambient temperature. Subsequently, a continuous profile is created by welding the two ends of the steel sheet together.

After the shaping process and profile formation, the steel undergoes further treatment through the hot-finishing process (Zhang et al., 2016). Both cold-formed and hot-finished profiles are subject to forming forces that induce plastic strain and can result in residual stresses, potentially leading to issues like fatigue and buckling. There is a preference for hot-forming profiles that do not undergo plastic straining during fabrication, thereby minimising residual stress (Zhang et al., 2016). Conversely, cold-formed profiles offer advantages in terms of ease and cost- effectiveness during fabrication (Zhang et al., 2016).

The manufacturing processes of both cold-forming and hot-forming can be directly applied to form CHS and smaller RHS (Southern African Institute of Steel Construction, 2016). However, for larger

RHS, an additional step involving the rolling of a circular section into a rectangular one is required (Wardenier, 2001). This process can be employed with either type of CHS, whether produced via hot or cold forming.

2.1.4 Material properties of Steel Hollow Sections

The design and structural performance of SHS are significantly influenced by the material properties of steel, which, in turn, are shaped by factors such as chemical composition, manufacturing processes, and overall quality. The elemental composition of steel primarily consists of iron, with minor proportions of carbon and other elements like manganese and vanadium. The carbon content in mild steel typically falls within the range of 0.1% to 0.25%. Higher carbon content contributes to increased strength and hardness but renders the steel more brittle. Conversely, steels with lower carbon content exhibit greater ductility, albeit with reduced strength, making them more amenable to welding. Mild steel is usually produced to maintain ductility, minimising the risk of brittle fractures, which are unfavourable due to their sudden and unexpected nature.

Structural steel, up to the yield stress (f_y), displays elastic behaviour following Hooke's Law. Beyond this point, it transitions into plastic behaviour, indicating permanent deformation. During this plastic phase, the steel undergoes work hardening, leading to excessive deformation before reaching the ultimate strength (f_u). It is important to emphasise that this elastoplastic behaviour is intrinsic to structural steel, whether subjected to tensile or compressive loads.

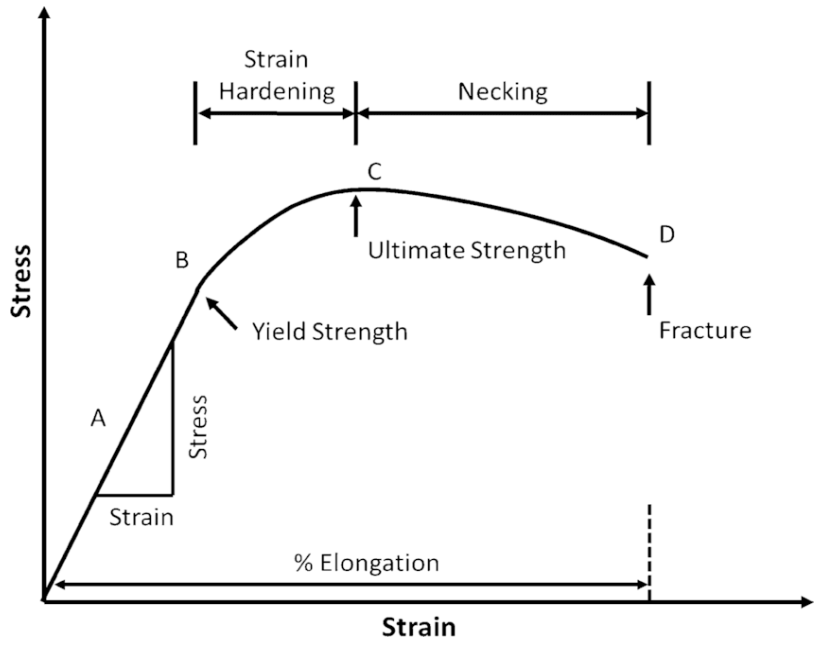

Figure 2-2 Stress strain curve (Lim & Hoag, 2013)

The SAISC Handbook (2016) indicates the properties and standards of structural steel which is used in HSS. These properties are given in Table 2-1.

Table 2-1 Material properties of steel used for HSS design, grade S355MH and S355J0H (SAISC,2016)

Property	Amount
f_y	355 MPa
f_u	450 MPa
M_OE	200 x 10^3 MPa
Density (ρ)	7850 kg/m^3
Poisson's ratio (υ)	0.30
G	77 x 10^3 MPa
Coefficient of expansion	11.7 x 10^{-6}/ºC
Specific heat (approximately)	480 J/kgºC
Thermal conductivity (approximately)	50 W/mºC

2.2 Ultimate Limit State (ULS) design of hollow sections

In South Africa, the design of SHS adheres to the relevant South African National Standards (SANS) guidelines. These codes employ a 'limit states' approach as the foundational framework for structural design. This approach necessitates the fulfilment of distinct limit states in the design process, encompassing the ULS, Serviceability Limit State (SLS), and Fatigue Limit State (FLS) (Parrott, 2014).

The ULS relates to the structural condition where the system faces the risk of collapse or considerable damage under the application of maximum loads. In contrast, the SLS arises when the structure is considered damaged or compromised due to excessive deflection, cracking, or vibration, rendering it potentially unsuitable for its intended use.

FLS are primarily associated with the potential for fatigue-induced failures and predominantly apply to structures subjected to varying live loads that induce cyclic stress variations. These may include structures supporting cranes that operate intermittently or continuously. In the scope of this study, the investigation into the effects of damage on SHS behaviour is confined to the ULS.

2.2.1 Design of hollow sections

SHS are purposefully designed to function as tension, flexural, or compression members, each requiring a distinct design approach. The design and structural assessment of these members are governed by specific standards and codes. For hot-formed steel members, compliance with SANS 10162-1 is imperative, while the design of cold-formed steel members follows the provisions outlined in SANS 10162-2. The segmentation of design methods and standards stems from the inherent differences in the characteristics of these members.

Cold-formed steel members are typically characterised by thin plates, often placing them within the classification of class 4 members. This classification recognises their susceptibility to local buckling phenomena, warranting the establishment of a separate design code. The adoption of distinct design methodologies and standards ensures the precise and tailored treatment of both hot-formed and cold-formed SHS members, optimising their structural performance.

2.2.1.1 Design of hollow section in tension

The design process for Square Hollow Section members subjected to tensile ultimate stress involves a meticulous assessment of their capacity to withstand tensile forces. Whether hot-formed or cold-formed, the objective is to ensure that the calculated resistance surpasses the force acting on the element, thereby preventing failure. Tensile components are susceptible to three distinct modes of failure: gross section yielding, net section rupture, and block shear failure, primarily due to tension and shear forces. Among these modes, the element's resistance hinges on the lowest

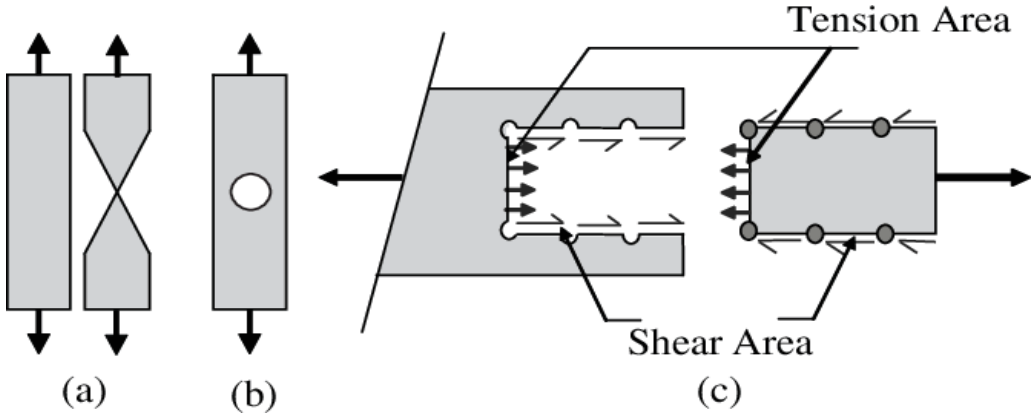

value determined from the analysis. The strength of HSS members is an amalgamation of factors, including their yield strength, cross- sectional characteristics, and a segment of the factor of safety employed. To compute the resistance of the element for any of these three failure modes, designated standards like SANS 10162-1 and SANS 10162-2 are enlisted. These standards provide the essential guidelines and methodologies to rigorously calculate the element's resistance under tensile ultimate stress, ensuring the structural integrity and safety of HSS members.

Figure 2-3 Tensile failure modes (Priya et al, 2011)

(a) Gross section yielding

(b) Net section rupture

(c) Block shear

2.2.1.2 Design of hollow section in compression

When designing Square Hollow Section compression members, a crucial aspect is to calculate the element's factor resistance to the compressive force and compare it to the actual compressive force acting on the member. Compressed SHS members are susceptible to various modes of failure, including local warping, warping, or flattening of the member. Typically, member warping tends

to occur before flattening, except in the case of noticeably short and stout members. The failure mode, whether buckling or material yield, is contingent on the member's slenderness ratio. Short columns, characterised by a low slenderness ratio, fail due to material yield, while long columns with a high slenderness ratio are more prone to buckling.

The design process for compression elements typically comprises two stages. In the initial stage, the cross-sections of the members are evaluated, often through a local buckling test. Subsequently,

in the second stage, the analysis determines the buckling and compression resistance of the component. The choice of method employed depends on whether the part passes or fails the local buckling test. In instances where parts fail the local buckling test (i.e., they are susceptible to local buckling), they are subject to separate design procedures as outlined in accordance with SANS 10162-2. This specialised approach accounts for the lower resistance exhibited by parts that do not meet the local buckling criteria.

2.3 Damage to hollow sections

2.3.1 Damage experienced by hollow sections

In the construction industry, structural elements that incur damage pose a significant and pressing challenge. This issue not only contributes to project delays but also escalates costs and compromises the overall safety of the structure (Mirambell, 2004). Steel structures are susceptible to a diverse array of damage types throughout their entire design life, affecting them at various stages. Some of the most popular types of damage are (Mirambell, 2004):

Table 2-2 Types of steel damage

Damage	Image	Cause	Outcome
Corrosion damage	 (Apostolopoulos & Koulouris, 2020)	Oxidation of steel	● Loss of material in the form of rust. ● Reduces the cross section of the element. ● Leads to a decrease in the load-bearing capacity.
Fragile fracture	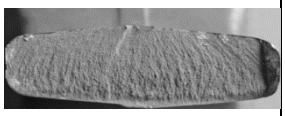 (Moore & Booth, 2015)	Negligible amount of plastic strain	● Leads to cracking, these cracks occur under specific conditions such as low temperatures or around areas where stress is concentrated.

Damage	Image	Cause	Outcome
Fatigue failure or Fatigue crack	 (Alithari, 2014)	• Occurs when members are subjected to different load cycles or no prior plastic deformation. • Usually begins with irregularities or defects such as nicks, dents, fire damage - high temperature caused by fire.	Changing the properties of steel, leading to deformation of steel elements, wrong member which can cause impacts of collisions, settlement of foundations and earthquakes can cause steel structures to be deformed or displaced from their original positions. Local defects usually in the form of nicks, grooves, and indentations, are often caused by accidental loads applied to the structure during construction or the life of the structure.
Dent damage	 (Dubinskiy et al., 2019)	• Occurs when members are subject to damage between fabrication and erection. Dent damage usually occurs during the transportation of the member.	These damage-induced imperfections on members may lead to a reduction in strength of the member. According to the SANS2001-CS1 (4.6.1.2), these damaged hollow sections need to be replaced.

2.3.2 Damage to hollow sections between fabrication and erection

Like traditional steel structures, Square Hollow Section components face susceptibility to the damage categories outlined in Table 2-2. Throughout the phase spanning fabrication to erection, SHS members are prone to localised imperfections. Within the realm of SHS, these imperfections commonly manifest as nicks, holes, and dents. In the context of SHS, the prevalent form of damage often manifests as dents. This tendency is attributed to the structural characteristics of SHS, where corners are securely fixed and rounded, reducing the probability of other types of imperfections stemming from inherent edges in SHS.

2.3.3 Causes of dent damage between fabrication and erection in hollow sections

The incidence of dent damage to Square Hollow Section members during the period between fabrication and erection varies depending on the nature of the structure under consideration. In the context of offshore structures, such as oil rigs, indentations in HSS components, both during and

after construction, are often ascribed to factors like ship impacts and falling objects, as previously highlighted in research (Godoy, 1996).

For other types of structures, dents typically result from various factors, including collisions with vehicles, improper storage of assemblies, and incidents during the transportation of assemblies to the construction site. Despite the high torsional stiffness characteristic of HSS, its multiaxial flexural, tensile, and compressive strength render it susceptible to damage without significant distortion, as documented in existing literature (Dutta et al., 1998). The potential for dent damage is a tangible concern.

To address the risk of damage during transportation, storage, assembly, and installation, precautionary measures such as careful packaging and supervised unloading are diligently implemented. However, it is crucial to acknowledge that, despite these efforts, dents can still occur.

2.3.4 Dent damage characteristics

While collisions often exhibit similar shapes, as depicted in Figure 2-4, the precise configuration of impacts can vary significantly based on factors such as the object's shape, the magnitude of the impact force, and additional variables. The formation of dents can also be influenced by residual stresses inherent in cold-formed members, as highlighted in previous research (Padula & Ostapenko, 1988).

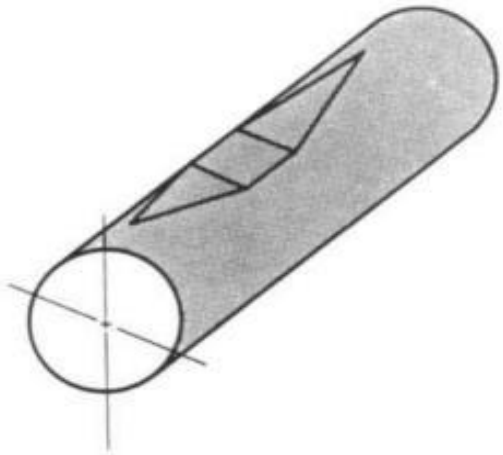

Figure 2-4 Dent on a circular hollow section (Godoy, 1996)

Dent geometry is diverse and can encompass shapes such as "V" shaped, flat, or round, as documented in the work of Padula & Ostapenko (1988). The complexity arises from the fact that many dents exhibit a combination of these geometric shapes, making precise classification challenging. Studies focused on dent analysis often resort to mathematical formulas to approximate dent shapes, as opposed to conducting a meticulous examination of actual dents.

This classification of dents can indeed be intricate, as by Kachanov (1986). Indentation damage fundamentally pertains to the alteration of material in a plastic state, rendering it incapable of supporting loads. This reduction in the cross-sectional area of the member available for load-bearing

purposes leads to the eccentric behaviour of axial loads, as articulated by Pacheco & Durkin (1988). Stress concentrations tend to occur in the undamaged portions surrounding the dented area, resulting in higher stress levels compared to the undamaged regions.

2.3.5 Effect of dent damage on hollow sections

In the late 20th century, studies were conducted to analyse and report on how structural performance was impacted on by indentation of HSS.

These studies were in axial compressions, lateral loading and/or flexure. A summary can be found in Table 2-3.

Table 2-3 Previous studies on structural performance by HSS

Study	Summary
Ultimate Strength of Damaged Tubular Bracing Members by C.P. Ellinas (1984)	Investigated offshore structures and the application in of CHS by method of developing analytical equations.
An Analytical Method for Predicting the Ultimate Capacity of a Dented Tubular Member by S. Durkin (1987)	Investigated offshore structures and the application of CHS by experimental data and FEA.
Denting and Collapse of Tubular Members- a Numerical and Experimental Study by L.A. Pacheco and S. Durkin (1988)	Investigated offshore structures and the application of CHS by experimental data and FEA.
Indentation Behaviour of Tubular Members by J.A. Padula & A. Ostapenko (1988)	Investigated offshore structures and the application of CHS by experimentation and FEA.
Laboratory Testing of Ultimate Capacity of Dented Tubular Members by E. Landet & I. Lotsberg. (1992)	Investigated offshore structures and the application of CHS by experimentation.
Moment-Curvature Relationships for Dented Tubular Sections by L. Duan, J.T. Loh &W.F. Chen (1993)	Investigated offshore structures and the application of CHS by experimental data.
Structural Characteristics of Damaged Offshore Tubular Members by S.R. Cho, J.S. Kwon & D.I Kwak (2010)	Investigated offshore structures and the application of CHS by experimentation.
Ultimate Strength of Locally Damaged Steel Stiffened Cylinders under Axial Compression by B.C. Cerik (2015)	Investigated offshore structures and the application of CHS by FEA.
Fatigue Tests of Damaged Tubes under Flexural Loading by T.G. Ghazijahani, H. Jiao &D. Holloway (2015)	Investigated offshore structures and the application of CHS by experimentation.

Methods have been systematically developed, drawing insights from these extensive studies to effectively model dent damage leveraging Finite Element Analysis (FEA) and analytical relationships. These advancements hold potential to enhance our comprehension of the intricate indentation processes, particularly the interplay between lateral force and indentation depth. As a result, the task of determining the residual strength of a damaged SHS has been significantly simplified. This is made possible through the utilization of specially crafted ‘designer’ analytical; formulas that have emerged as a direct outcome of these research endeavours.

2.3.6 Effects of dent damage on ultimate strength of axially loaded HSS

Methods informed by insights gleaned from extensive studies have been systematically developed to model dent damage, employing both FEA and analytical relationships. These advancements hold the potential to enhance our understanding of the intricate indentation processes, with a particular focus on clarifying the relationship between lateral force and indentation depth. As a result, the determination of the residual strength of a damaged Square Hollow Section has been significantly simplified. This efficiency is achieved through the application of specialised 'designer' analytical formulas that have emerged directly from these research endeavours. Smaller-sized dents in HSS can weaken the ultimate strength of CHS. For instance, research indicates that a dent with a depth of 8.5mm can result in a substantial 30% reduction in the ultimate strength of a 100mm diameter CHS (Pacheco & Durkin, 1988).

Numerous studies conducted by Ellinas (1984), Durkin (1987), and Pacheco & Durkin (1988) consistently yield similar findings regarding the impact of damage-induced imperfections on the ultimate strength of CHS.

2.4 Existing requirements for dent damage repair in hollow sections

The SANS Code 2001-CS1(2005): Structural Steelwork plays a pivotal role as a crucial reference, defining construction requirements for the manufacturing and erection of structural steel. Within the code, Clause 4.6.1.1, falling under the domain of storage and processing, mandates that steel members undergo processing and storage practices that minimise the probability of surface wear and damage. In concordance with this, Clause 4.6.1.2 of the code specifies that any steel structures damaged during unloading, storage, transportation, or assembly must undergo restoration to conform to the prescribed manufacturing guidelines. Table 3 of the SANS Code 2001-CS1(2005) provides additional permissible deviations in rolled components post-manufacture, encompassing parameters such as tip preparation, curve, straightness, length, and twist in both axes. However, it is essential to highlight that the code does not address localised defects such as cracks, dents, and holes.

In cases where structural elements are affected by these defects, the code recommends their transfer to a factory, as per Clause 4.6.1.2. When damage is identified, the code dictates that the damaged section should be 'restored' to meet the manufacturing standards outlined in SANS 2001-CS1 (SANS, 2012). Nevertheless, it is important to note that the code lacks scientific references or explanations to substantiate this approach. This may potentially result in unwarranted repair or

replacement of dented components, incurring substantial costs, causing disruptions, and leading to significant construction delays. The manufacturing standards outlined in SANS 2001-CS1 include tolerances, forming an integral part of the regulatory framework.

1. Part tolerances for SHS that is cold-formed: For cold-formed SHS, SANS Code 2001-CS1(2005) aligns with SANS 657-1, defining stringent part tolerances. These tolerances encompass critical parameters such as external dimensions, ovality, thickness, and squareness, which cold-formed SHS must adhere to.
2. Section tolerances for SHS that is hot-formed: In the case of hot-formed SHS members, SANS Code 2001-CS1(2005) defers to EN 10210-2 as its guiding standard. The code extends the same tolerances applicable to part parameters, mirroring those stipulated in SANS 657-1, for hot-formed SHS as well.
3. Tolerances of other Members: Beyond the cross-sectional dimensions, SANS Code 2001-CS1(2005), in Table 3, depicts a comprehensive array of tolerances that encompass various aspects of SHS members. These extend to parameters such as part straightness, a facet that can also be significantly influenced by the presence of indentations.

Table 1 of SANS Code 2001-CS1(2005) encapsulates the relevant terms and clauses from the reference codes. British Standard BS EN 10210-2:2006 and BS EN 1090:2008+A1:2001 do not provide explicit guidance on prescribed procedures for handling damaged structural members. In contrast, both the Australian standard AS 4100-1998 and the Canadian standard CSA S16-09:2009 closely align with the principles outlined in SANS Code 2001-CS1(2005). These standards emphasise the importance of processing, storing, and transporting members in a manner that prevents any harm to these components.

In addition, in AS 4100-1998, which specifies that an item, even if manufactured with a defect, may still be considered acceptable if it can be convincingly demonstrated that the structural capacity of the item remains uncompromised. This approach recognises the potential for acceptance of items with defects, provided their structural integrity is verified.

2.5 Modelling damage-induced imperfections

The configuration of resulting indentations typically displays a complex nature, influenced by various factors such as the geometry of the impacting object, the cross-sectional profile of the component, its orientation, and the force of impact generating these dents (Elias, 2020). As a result, the shapes of these indentations, commonly referred to as dents, often exhibit intricate patterns that prove challenging to accurately categorise and replicate for analytical purposes. In scientific investigations, researchers frequently resort to simplified idealisations that can be conveniently reproduced in laboratory settings or within finite element software.

Studies such as those conducted by Padula & Ostapenko (1988), delved into dent shapes within CHS and considered configurations, including V-shaped, rounded, and flattened dents at the centre of CHS profiles. Meanwhile, research by Tan et al. (2015) specifically examined dents within SHS, with a focus on the V-shape configuration, as depicted in Figure 2-5.

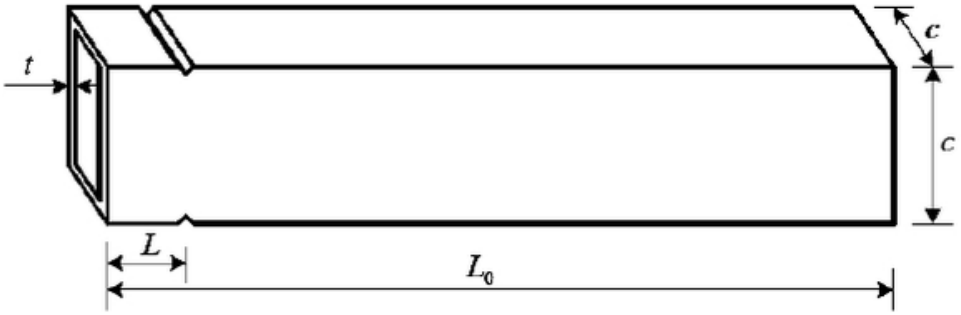

Figure 2-5 Typical V-shape dent (Tan et al., 2015)

Other studies such as (Wu et al., 2017) and (Prabu et al., 2010) consider the complex dent shape of CHS, as shown in Figure 2-6.

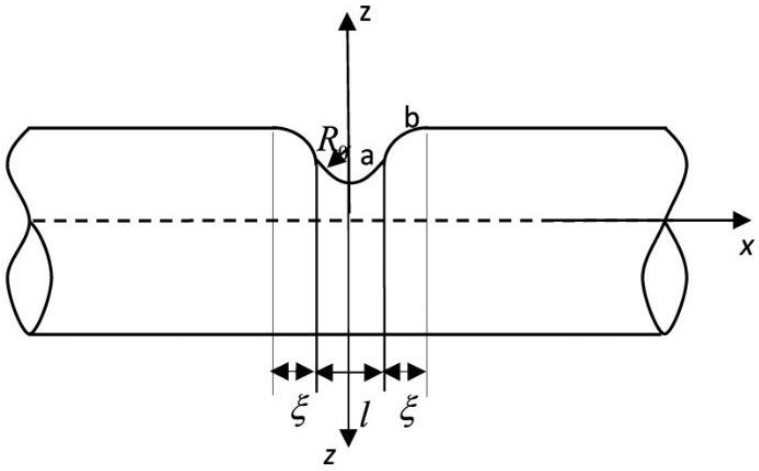

Figure 2-6 Typical rounded dent on CHS (Wu et al.,2017)

It is established that the region within an indentation undergoes plastic deformation, leading to irreversible damage, even when the shape of the indentation varies. Significantly, as explained by Ellinas (1984), this phenomenon results in a reduction of the modulus of elasticity (E) within the indented section, leading to axial loads acting eccentrically. These deviations ultimately contribute to a lower load-bearing capacity. Effectively modelling the shape of the indentation requires a comprehensive consideration of material behaviour within the indented region, albeit with reasonable assumptions. This involves balancing factors such as analytical complexity, computational demands, and result accuracy.

It is considered that the buckling of the cross-section due to the damaged area is negligible and is therefore, often omitted during modelling, as proposed by Cerik (2015). Various methodologies have been proposed to describe dent damage in terms of both geometry and material properties, with three overarching approaches governing the consideration of material properties within the indented zones.

Method 1: *Alter Material Properties in Indented Areas*

This approach entails a reduction in elastic modulus and elongation, as explored by Ellinas (1984), with steel strength typically lowered to 50-75% of its original value. While straightforward, this method provides a reasonably accurate estimation of the structural strength impact resulting from dent damage.

Method 2: *Disregard Material Within the Indented Area*

A further simplification of Method 1, this technique, adopted by Elias (2020), involves excluding compliant steel within the indented region without adjusting Young's modulus and yield strength. It operates under the assumption that the plastically deformed concave portion becomes ineffective, and the load is borne by the active section of the concave part, in line with Ellinas (1984) perspective. This approach simplifies finite element modelling while yielding reasonably accurate outcomes.

Method 3: *Maintain Material Properties in the Indented Area*

Under this method, material properties within the indented zones remain unchanged. The predominant focus is on geometric imperfections, as this process preserves material properties. This approach is particularly advantageous in simplifying FEA, particularly when researchers primarily concern themselves with geometric instabilities.

Regarding the representation of dent shapes, two prevalent methodologies are commonly employed:

Method 1: *Express Dent Shape Utilising Formulas*

This technique relies on simplified mathematical formulas to depict the three-dimensional shape of the dent. These formulas often leverage cross-sectional component properties, such as radius, perimeter, and thickness, to describe the geometry of the dent. The resulting equations may manifest as V-shaped dents, sinusoidal waves, or straightforward linear equations, including exponential decay equations in both longitudinal and transverse dimensions. Works by Prabu et al. (2010), Cerik (2015), and Padula & Ostapenko (1988) provide a comprehensive insight into these equations.

Method 2: *Employ Circular Cutouts to Represent Dents*

Here, the indentation shape is symbolically portrayed as a circular cross-section, with the size of the dent expressed as the ratio of the hole's radius to the component's circumference. This approach effectively disregards material properties within the indented region, grounded on the presumption that the yielding material in this region is incapable of withstanding stress.

2.6 Analysis of linear and non-linear methods, of HSS, to determine their buckling capacity

Buckling analysis is a foundational aspect of structural engineering aimed at predicting the behaviour of structures under loads, especially in situations where instability or buckling is a

concern. Two primary methods are commonly employed for conducting buckling analysis (linear buckling analysis and non-linear buckling analysis).

2.6.1 Linear Buckling Analysis (LBA)

LBA is a widely employed method for predicting the theoretical critical buckling loads of structures, assuming linear elastic material behaviour. This analysis can be carried out manually or with the aid of FEA software. A common approach for calculating the critical linear buckling load involves the application of Euler's buckling load equation. Euler's equation offers an estimate of the critical load at which a slender structural member becomes unstable and undergoes buckling. The general form of Euler's buckling load equation is as follows:

Where:

$$P = \frac{\pi^2 EI}{(KL)^2} \quad \text{..... (2-1)}$$

- P is Euler's critical buckling load.
- E is the Young's Modulus of the material.
- I is the second moment of area of the section.
- L is the length of the member.
- K is the effective length factor.

Equation 2-1 Euler's critical buckling load

In FEA, when the primary load deflection path is influenced by secondary load deflection paths, LBA is employed to calculate the critical load at which structural instability, such as buckling, occurs (Prabu et al., 2010). This method provides Buckling Load Factors (BLF) for different buckling modes and is computationally efficient, making it a preferred choice for many engineering applications due to its speed and resource efficiency. However, LBA has limitations as it assumes linear behaviour and neglects non-linearity, making it unsuitable for structures with non-linear characteristics or imperfections.

It is essential to note that LBA does not yield numerical values for the displacement caused by the buckling load, and therefore, it cannot be used to determine the post-buckling behaviour of the structure (Elias, 2020). Moreover, LBA does not accurately predict buckling loads for structures that are imperfect or sensitive to non-linearity (Ellobody et al., 2014). When dealing with structures exhibiting imperfections or sensitivity to non-linearity, engineers often resort to other analysis methods for more precise predictions of buckling loads and behaviours.

2.6.2 Non-linear buckling analysis

Non-linear buckling analysis is employed to predict the buckling strength of a member by considering the non-linear relationship between applied loads and resulting displacements,

stemming from both geometric and material factors. In this analysis, conducted using finite element software, loads are incrementally applied, and at each stage, a stiffness matrix is computed to determine when the structure becomes unstable (Prabu et al., 2010).

During non-linear analysis, increments for load application can be either user-defined or automatic, aiming to minimise the displacement difference between consecutive load increments. However, in buckling analyses, this approach can be challenging, as the structure loses stiffness and becomes unstable once buckling occurs. To address this, finite element software often incorporates the arc length method to control load application, enabling solutions even in the presence of instability. For example, ABAQUS software offers the Riks method, a modified arc length method, for non-linear buckling analysis.

Non-linear analysis considers both material and geometric non-linearities, making it the preferred method for assessing the buckling strength of imperfect bars. In contrast to LBA, non-linear analysis provides stress and displacement data, facilitating a comprehensive understanding of the structure's behaviour after buckling. However, it comes with trade-offs in terms of complexity, increased computation time, and greater computational resource demands compared to LBA.

2.7 Conclusion of literature review

Dent damage has the potential to significantly influence the structural performance of SHS with its impact being influenced by factors such as indentation shape and the specific type of SHS part. Typically, HSS members are manufactured and transported as subassemblies before construction, rendering them susceptible to various forms of damage. However, the current approach outlined in SANS Code 2001-CS1(2005) for repairing dent damage to HSS components appears to lack a scientific foundation, potentially resulting in unnecessary repairs or replacements that contribute to cost overruns and construction delays.

Much of the existing literature on dent damage primarily focuses on circular rather than square or rectangular hollow sections. Nonetheless, insights from CHS literature suggest that SHS may encounter significant challenges due to dent damage. To enhance current practices, establishing tolerances that specify acceptable damage levels is a viable option. However, it is crucial to recognise that even relatively small dents can reduce the strength of damaged HSS elements, indicating that relying solely on manufacturing tolerances may not be sufficient.

In summary, addressing dent damage in SHS necessitates further research and the development of refined practices to efficiently ensure structural integrity. This involves considering specific factors related to SHS, understanding the implications of dent damage, and establishing more comprehensive guidelines that go beyond current standards.

3. Research Methodology

The objectives of the research were met using the methods summarised in Figure 3-1 below.

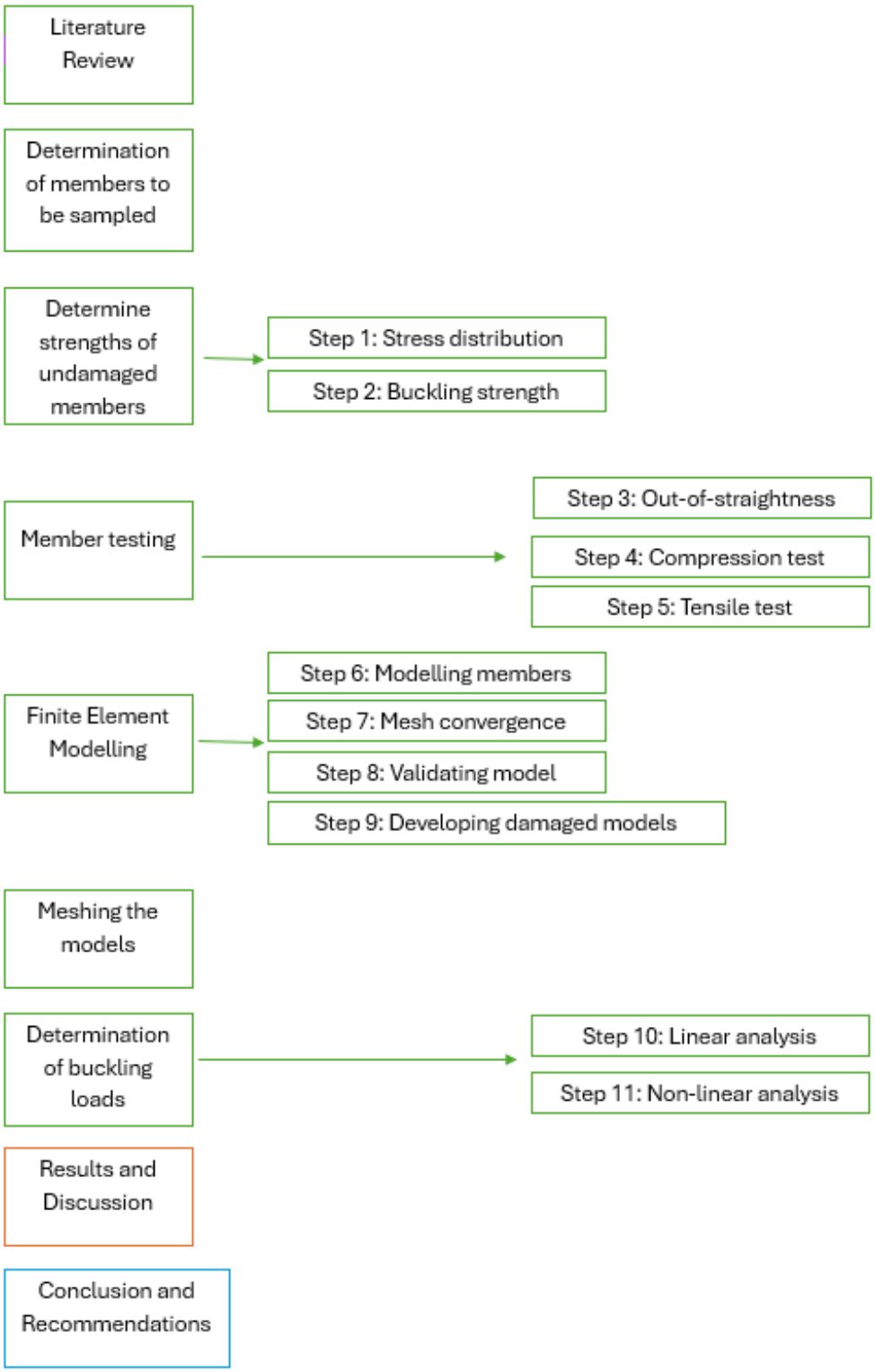

Figure 3-1 Method of study

3.1 Literature Review

The preliminary phase of this study involved a literature review aimed at gaining a comprehensive understanding of the existing body of work. This encompassed exploring the historical context, manufacturing processes, effects of dent damage, and diverse applications of steel hollow sections. Additionally, the review explored linear and non-linear buckling behaviours exhibited by steel hollow sections, scrutinising technical facets such as material properties and geometric considerations.

The investigation extended to the contemporary utilisation of hollow sections in various industries, shedding light on their current applications. Furthermore, the study investigated the limitations and tolerances associated with hollow sections when subjected to damage, as outlined in the SANS codes of practice. This comprehensive literature review served as a foundational step in establishing an understanding of the historical, technical, and practical aspects related to steel hollow sections, paving the way for subsequent stages of the research.

3.2 Determination of members to be sampled.

The second phase of this study involved determining the dimensions, sizes, and quantity of hollow sections to be included in the testing process. SHS are typically manufactured in standardised sizes, and relevant information can be found in section 2.1.5 of the South African Steel Handbook (Southern African Institute of Steel Construction, 2016). However, due to the constraints of the study, not all hollow sections listed in the handbook could be tested. To gain a more focused understanding of the impact of damage on hollow sections, a single size and type of hollow section are selected for testing.

Nine SHS with dimensions of 50 x 50 x 4 mm were chosen as the samples for testing. The selection was made based on the limitations of the testing equipment, which imposed a maximum height of 450mm for the sections. Among these nine samples, six were intentionally damaged, while three remained undamaged. To facilitate testing, each hollow section was welded to an end plate at both ends, with the end plate having dimensions of 150 x 150 x 10. This approach allowed for a targeted examination of damage effects on a specific type and size of hollow section within the defined constraints of the study.

Figure 3-2 shows the fabricated hollow sections. The dimensions and technical drawings can be found in Appendix A1.

(a) Undamaged specimens (Type A)

(b) Damaged Specimens (Type B)

(c) Damaged Specimen (Type C)

Figure 3-2 Square hollow section samples

Table 3-1 Member samples of hollow sections to be tested

Member Label	Type of hollow section	Dent Size (mm)	Dent position (distance from base in mm)	h x b x t (mm)	Length (mm)
Undamaged					
A1	Square	25	N/A	50 x 50 x 4	450
A2	Square	25	N/A	50 x 50 x 4	450
A3	Square	25	N/A	50 x 50 x 4	450
Damaged					
B1	Square	25	Centre (225)	50 x 50 x 4	450
B2	Square	25	Centre (225)	50 x 50 x 4	450
B3	Square	25	Centre (225)	50 x 50 x 4	450
C1	Square	25	Quarter distance from base (112.5)	50 x 50 x 4	450
C2	Square	25	Quarter distance from base (112.5)	50 x 50 x 4	450
C3	Square	25	Quarter distance from base (112.5)	50 x 50 x 4	450

The hollow sections listed in Table 3-1 were slated for testing in the Amsler compression machine. Additionally, tensile tests were conducted on the steel. To facilitate these tensile tests, six dog bone samples were extracted from the excess material remaining after cutting the nine samples designated for testing. From this surplus material, three samples were cut from the face of the section, and another three samples were cut from the corner of the section. A visual representation of these dog bone samples can be found in Figure 3-3, guiding the placement and orientation of the samples for the tensile testing process. This comprehensive testing approach aims to provide a thorough assessment of both compression and tensile behaviours of the selected hollow sections. The dimensions and technical drawings of the dog bone samples can be found in Appendix A2.

(a) Tensile Coupon specimens

(b) Corner specimens

Figure 3-3 Dog bone samples

3.3 Determine strengths of undamaged members

The assessment of the impact of damage on hollow sections necessitates an understanding of their undamaged strengths. Given that both tension and compressive experimental testing were conducted on the specimens, it is necessary to consider both compressive and tensile strengths in the calculations.

The yield or tensile strength of a SHS, representing the maximum load the material can sustain before reaching its yield stress, is equal in both compression and tension. This research study focuses on determining the buckling strength of the members, which can subsequently be used to derive the strengths.

Euler's buckling load is employed to calculate the buckling strength of a member. By establishing the yield strength and buckling strength, this study aims to provide comprehensive insights into the mechanical behaviour of the hollow sections, laying the foundation for a thorough evaluation of damage impact through experimental testing.

3.3.1 Stress distribution (step 1)

To determine the yield strengths; first the load at which the steel section yielded must be determined. Equation 3-1 was used to determine the load that undamaged sections, with uniform cross-sections, by multiplying the cross-sectional area by the yield stress of the steel section.

$$F_{uy} = f_y \text{ x A} \quad \text{.....(3-1)}$$

Where:

- F_{uy} yield strength of undamaged member
- f_y yield stress of the member
- A cross-sectional area of the member

Equation 3-1 Yield strength

3.3.2 Buckling strength (step 2)

The Euler buckling equation shown by Equation 3-2 was used to calculate the buckling strengths of the undamaged members. The members were modelled with fixed ends as these conditions were used for experimental testing.

$$F_{ub} = \frac{\pi^2 EI}{(KL)^2} \quad \text{..... (3-2)}$$

Where:

- F_{ub} buckling strength of undamaged member E modulus of Elasticity
- I second moment of area L length of the specimen
- K effective length factor (where K = 0.5)

Equation 3-2 Euler buckling

Table 3-2 Yield and buckling strength of undamaged members (based on Equations 3-1 and 3-2)

Member	Yield Strength (kN)	Buckling Strength (kN)	Compression Failure Mode
SHS	232.25	96.65	Buckling

3.4 Member Testing

Testing of the SHS were carried out in three parts, namely the out-of- straightness test, compression test and tensile coupon test.

3.4.1 Out-of-straightness test (step 3)

To determine any deflections of the untested members, an out-of-straightness test was carried out using the set up shown in Figure 3-4.

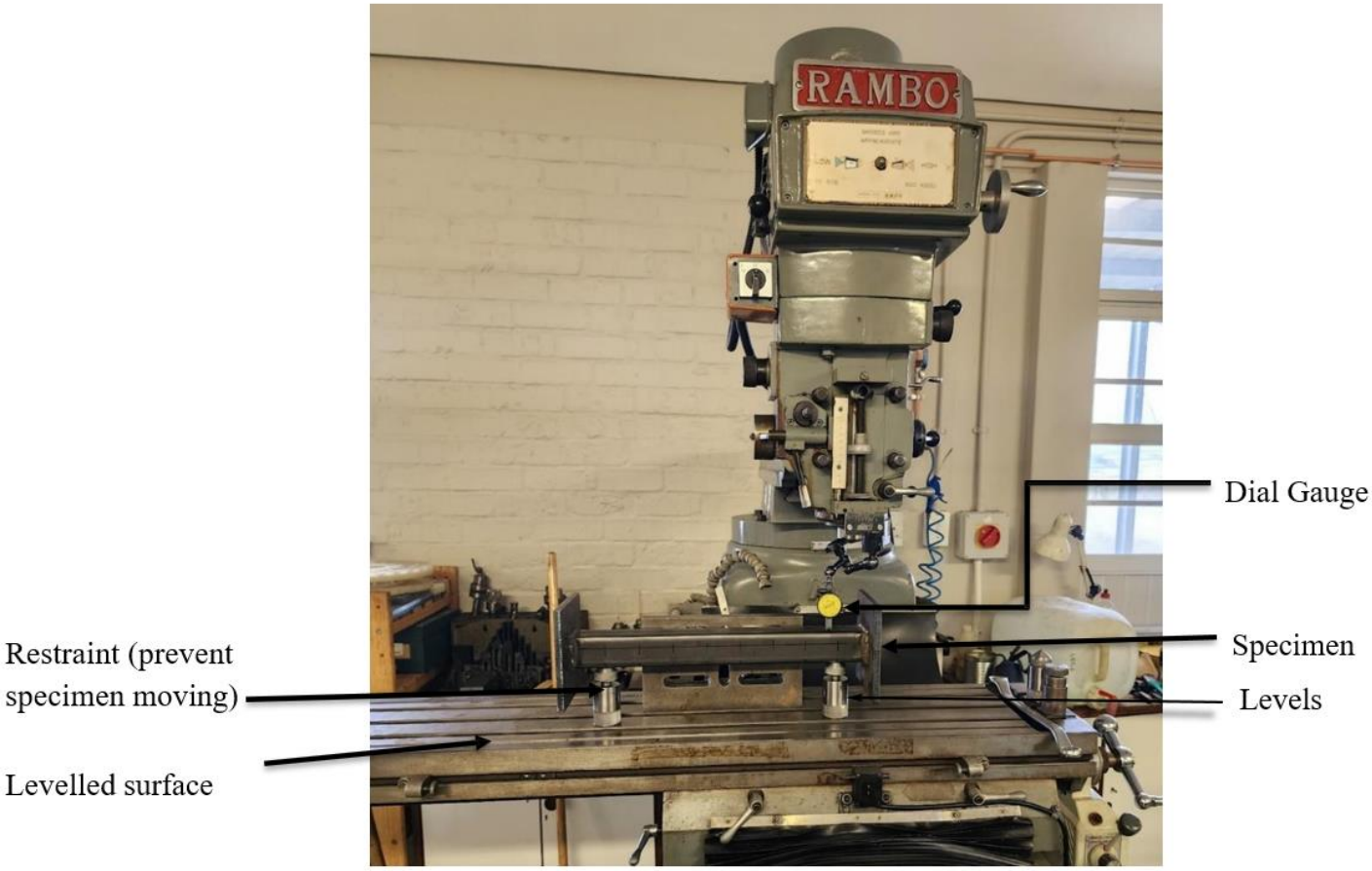

Figure 3-4 Out-of-straightness testing set up

The specimen was seated on a pair of levels which were placed on a levelled work surface. The dial gauge was zeroed on the right end as shown in Figure 3-4 and Figure 3-5.

Figure 3-5 Zeroed dial gauge

The dial gauge had a start at a 50mm offset distance from the base of the hollow section. Readings were taken at 50mm intervals whereby the dial gauge was run across the centre of the flat face of the specimen to the far end where it was levelled to zero as well. The dial gauge was then run across the length of the specimen and the out-of-straightness results were read and recorded, as shown in Appendix B. This process was done in both the x-x and y-y direction for each of the hollow section specimens.

3.4.2 Compression test (step 4)

Compression tests were carried out using the Amsler machine shown in Figure 3-7. Prior to testing, the mass of each specimen was found using the scale shown in Figure 3-6.

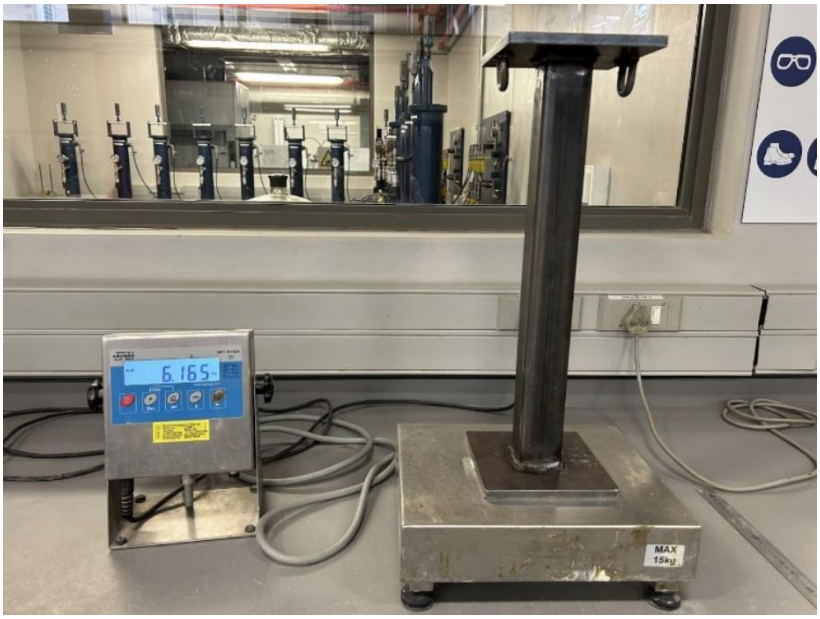

Figure 3-6 Mass of hollow section

Figure 3-7 Amsler testing machine

Each of the nine hollow section specimens underwent compression testing in the Amsler machine. A load, applied at a rate of 0.39 - 0.79 kN/s, was exerted onto the hollow sections until the point of maximum failure load. A dial gauge was set up, zeroed, and affixed to the plate of the Amsler to precisely measure the outward deflection of the hollow section during compression.

As a safety precaution, ratchet ropes were employed to restrain the hollow sections. This measure was implemented to prevent any movement or potential displacement of the hollow section, commonly referred to as 'popping out' of the machine, during the compression process. Figure 3-8 and Figure 3-9 provide a visual representation of the setup for specimen A1 both before and after compression, highlighting the safety measures in place during the testing procedure.

Figure 3-8 Specimen A1 before testing

Figure 3-9 Specimen A1 after testing

The mass of the specimens as well as the results from the compression tests can be seen in Table 3-3 below.

Table 3-3 Mass, load, and deflection of specimens

Member Name	Mass (kg)	Load (kN)	Location of Max Deflection from base (mm)	Max Deflection (mm)
A1	6.165	325	225	13.211
A2	6.150	325	220	13.509
A3	6.105	330	250	8.000
B1	6.115	274	225	9.963
B2	6.135	281	227	5.529
B3	6.145	282	225	6.892
C1	6.165	296	112	5.436
C2	6.110	294	112	5.343
C3	6.140	285	110	5.259

When testing was carried out, it should be noted that specimen A3 had to be tested twice as the end plate was not flush with the loading seats of the Amsler, due to fabrication inconsistencies, which caused some uncertainties when tested. Figure 3-10 below shows the test samples after they were compressed.

(a) A1, A2, A3 after testing

(b) B1, B2, B3 after testing

(c) C1, C2, C3 after testing

Figure 3-10 Compressed specimens

From the readings of the Amsler testing, load displacement graphs were plotted and can be found in Appendix C.

3.4.3 Tensile test (step 5)

To conduct a tensile test, six dog bones were cut out from the excess hollow section material as seen in Figure 3-3. These dog bones were designed in accordance with SANS 6892 and the location of where the flat and corner specimens were cut from can be seen in Table 3-4. These specimens were tested in a Zwick1484 Universal Tester as seen in Figure 3-11 below.

Table 3-4 Flat face and corner cut out locations of dog bones

Dog bone	Location on SHS	Actual Specimen
Flat face	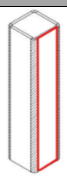	
Corner	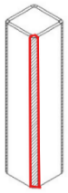	

Figure 3-11 Zwick1484 Universal Tester

Figure 3-12 Clamped flat face dog bone

The flat face dog bones were clamped into the machine as seen in Figure 3-12. A constant rate was applied onto the dog bones during the testing. The grips pulled the dog bones until a failure was reached as seen in Figure 3-13.

Figure 3-13 Failed specimen

The corner face dog bones were also tested in the Zwick1484 Universal Tester. However, due to the surface of the specimen being rounded and not flat, it required to be pinned to the plate for testing; as seen in the front and behind views in Figure 3-14.

(a) Front view (b) Behind view

Figure 3-14 Pinned connection for tensile testing

The results from the testing can be seen in Figure 3-15. The graph shows that the pinned corner specimens have a lower ductility but a higher yield strength whereas the fixed flat face specimens have a higher ductility but a lower yield strength. The test cross-sectional area of the corner specimen is much smaller. and hence the stress is higher. The average yield strength of the corner specimens was 409MPa versus 360MPa for the flat face specimens.

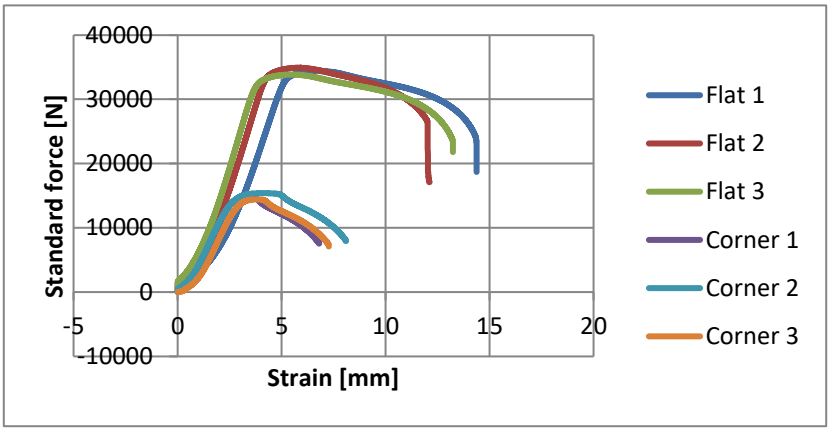

Figure 3-15 Stress-strain graph per tensile test results

Factors to note in the tensile testing included:

- Flat face specimens had a slight initial curvature which led to an observed 'drift' pf results (increasing strain with little tension force increase) before a pick up in the tension force with change in strain.
- Lack of an 8mm diameter pin to secure the corner specimens to the Zwick1484 Universal Tester which resulted in using a 7.5mm pin to restrain the coupon.

3.5 Finite Element Modelling

3.5.1 Modelling members (step 6)

Using the finite element modelling software, ABAQUS, the hollow section members were modelled as thin homogeneous shell elements, considering the small thickness of the sections in relation to their length and width. This choice resulted in the requirement for fewer nodes for each modelled specimen and reduced computational time. The specimens were designed with a middle-surface shell definition.

To mitigate large stress concentrations at the support perimeters, boundary conditions were applied to both ends of the member through interaction constraints. This involved defining a reference point at the centre of the cross-section at each support, followed by applying a rigid body constraint from the reference point to the perimeter of the cross-section. Subsequently, loads and boundary conditions could be applied at these reference points. Given that testing in the Amsler machine involved fully fixed conditions, the boundary conditions were defined as fixed as depicted in Figure 3-16 below. This modelling approach ensures a realistic simulation of the structural behaviour of the hollow sections during testing.

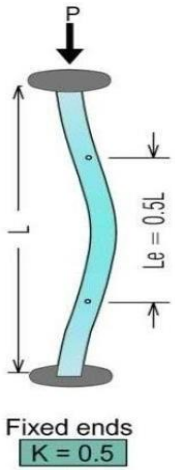

Figure 3-16 Fixed end condition setup

S4R elements, also known as linear quad elements, were used to provide uniform meshes in the member models. Excessive computational resources were not required. Each of the hollow sections had a thickness of 4mm. The member was then modelled with an evenly distributed thickness on the shell surface represented by ABAQUS.

3.5.1.1 Member model calibration

Correct calibration of a member model in finite element software typically yields fairly accurate results. The mesh size is a critical factor in influencing the accuracy of finite element results, and using smaller mesh elements increases mesh density, contributing to higher accuracy. While more accurate results are preferable, it is essential to consider the trade-off, as a model with more elements requires a longer time to solve.

In the modelling process using an ABAQUS license, there is a limitation on the number of nodes, impacting the model's complexity. Striking a balance between accuracy and computational efficiency is crucial. Hence, an optimal mesh size needs to be determined through a convergence study. This study aims to establish the mesh size for modelling the members, confirm the accuracy of the selected mesh sizes, and identify the point at which further refinement of the mesh no longer significantly alters the results. The convergence study helps ensure that the finite element model is both accurate and efficiently solvable within the constraints of the available resources.

3.5.2 Mesh convergence study (step 7)

In the mesh convergence study, a coarse mesh or large mesh elements are initially selected. The finite element model is then solved using the chosen mesh size, and this process is iteratively repeated with progressively smaller mesh sizes. The study continues until there is no longer a significant change in the results, indicating that the optimal mesh size has been determined.

The mesh convergence study in this research focused on linear buckling analysis applied to both undamaged and damaged SHS. The undamaged results were compared with theoretical results

obtained using the Euler buckling load equation (as described in section 3.3.2). The undamaged modelled results were also compared with experimental results presented in Table 3-3. For this, a non-linear analysis was conducted by inputting the initial imperfection from the analysis into the model. It is essential for the models in both linear and non-linear cases to be similar, as ABAQUS does not automatically check the compatibility of nodes between the two models. A separate mesh convergence study for the non-linear case was not required.

When conducting the convergence study, the following was observed:

- As the mesh size decreased, the solving time increased.
- As the mesh size decreased, there was a decrease in the percentage error between the linear analysis and the Euler buckling load.

The SHS modelled in Abaqus were both damaged and undamaged. Varying techniques were used when meshing the models, depending on the suitability of the technique, it was applied to the model or a part of the model.

3.5.2.1 Meshing techniques:

- Free technique is used for the meshing of all damage across medium and large members. It is also the most appropriate technique for smaller sized members with lower levels of damage as the size of the elements were larger when compared to the size of the damage.
- Structured technique is used for meshing as it applies mesh patterns that have been pre-established by the ABAQUS software onto the model. This technique also provides the most amount of control over your mesh because of the existing mesh patterns.

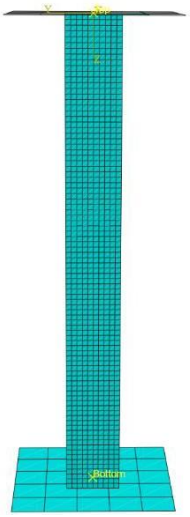

Figure 3-17 Undamaged free mesh

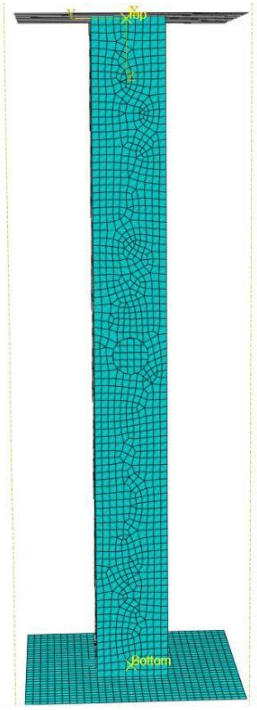

Figure 3-18 Centre dent free mesh

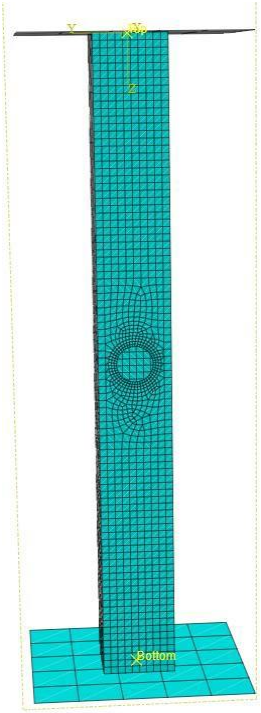

Figure 3-19 Centre hole structured mesh

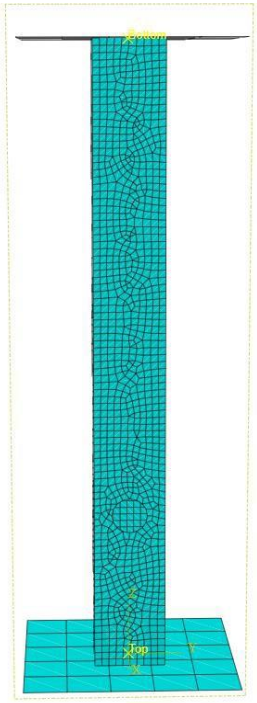

Figure 3-20 Off-centre hole fresh mesh

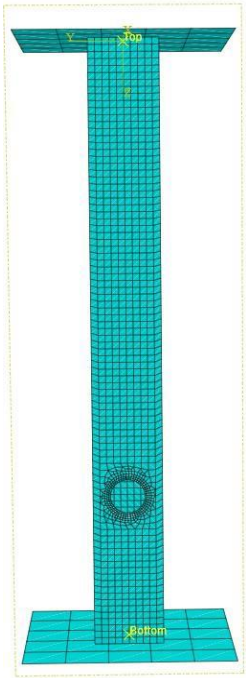

Figure 3-21 Off-centre hole structured mesh

3.5.3 Validating the model (step 8)

Post developing the mesh for the models, the models were fixed at the end points and a stress and linear buckling analysis were carried out. These results and the theoretical results were compared. This was done to compare the accuracy of the model.

3.5.4 Developing damaged models (step 9)

3.5.4.1 Modelling member geometry

In non-linear analysis using the Riks method, determining the post-buckling behaviour for perfectly straight members is challenging. This difficulty arises due to the discontinuous responses and instabilities that occur once the buckling point is reached. To observe the buckling response before reaching the load at which critical buckling occurs, a geometric imperfection is introduced to the initially perfect geometry of the model. This introduction of imperfection allows for a continuous response.

Table 3 of the SANS2001-CS1 provides the maximum permissible fabrication deviation, which serves as the basis for defining the imperfection in the model. By incorporating this imperfection, the non-linear analysis can capture the post-buckling behaviour and simulate the structural response beyond the point of buckling, providing a more realistic representation of the member's behaviour under loading conditions.

The code specifies the use of either:

- The larger of:

  $\frac{L}{1000}$ or 3mm

- The smaller of:

  $\frac{L}{500}$ or 25mm

In the case of the SHS used in this study:

$\frac{450}{1000} = 0.45\text{mm} < 3\text{mm}$, therefore take 3mm

$\frac{\mathbf{450}}{\mathbf{500}} = 0.9\text{mm} < 25\text{mm}$, therefore take 0.9mm

The 3mm imperfection, which was the larger of the two, was used. The actual measured tolerances from the out-of-straightness test confirmed the theoretical tolerances in the code, therefore the code standard specifications were used. The buckling mode, found from the linear analysis, determined the way the imperfection was added to model. Table 3-5 outlines the procedure used depending on the buckling mode obtained after the perfectly straight member was modelled and a linear analysis was conducted.

Table 3-5 Choice of imperfection introduction

Global buckling mode obtained (half-sine wave)	First eigen mode of the analysis was used as the initial imperfection for the non-linear analysis (this was scaled up by a 3mm imperfection)
Global buckling mode not obtained	Use of curved imperfection or out-of- straightness, in the form of a half-sine wave analysis, to create the non-linear model (3mm at the mid-section height)

When an imperfection was used in the model, the model and the mesh were copied. This was done to ensure that both the linear and non-linear model were similar.

3.5.4.2 Damage model

In Chapter 2, the literature review explored various methods of modelling damage, revealing intricacies in ABAQUS software regarding how to capture the hole profile on the software model, as discussed in studies by Cho, Kwon, and Kwak (2010) and Pacheco and Durkin (1988). The decision was made to model damage in the section using a hole as a simplified representation. This approach was chosen as when a hollow section is dented, the material enters the plastic region, resulting in a similar outcome to creating a hole. In both cases, the damaged portion of the material loses its ability to contribute to the member's strength and carry a load. This method is considered more accurate than decreasing the modulus of elasticity and yield strength in the damaged region, as proposed by Ellinas (1984). The dent geometry was applied by Elias (2020) for ease of modelling.

Six (6) out of the nine (9) specimens were intentionally damaged, and the location of this damage can be found in the technical drawings in Appendix A. The members in ABAQUS were modelled to have the same dimensions as the experimental specimens.

3.5.4.3 Location of the damage

The damages in both the testing specimens and the models were located at the midspan of the specimen and a quarter of the way from the bottom of the specimen. The assumption for choosing the midway location, as suggested by Cho, Kwon, and Kwak (2010) and Pacheco and Durkin (1988), is that damage located centrally would result in the most significant reduction in the member's strength and would be more critical. This hypothesis is supported by the testing results presented in Table 3-3.

It is important to note that damage was only considered to occur on the flat face of the specimens, as opposed to the corners. This choice was made due to constraints on funding for materials and for ease of modelling.

3.5.4.4 Hole sizes

To ensure consistency in results, the hole sizes for all specimens were kept uniform. While Pacheco and Durkin (1988) and Durkin (1987) explore a size parameter based on the ratio between the diameter of the specimen before damage and the hole depth, this study focuses on SHS, and thus, lacks a direct relationship between diameter and hole depth. Considering this, a non-dimensional parameter known as the size ratio—specifically, the ratio of the hole radius to the perimeter of the mid-surface prior to damage—was chosen as the method for sizing the damage, as proposed by Elias (2020). This approach provides a consistent and applicable means of characterising hole sizes in the context of SHS.

3.5.4.5 Yield strength of damaged members

After introducing the damage into the model, the yield strength was determined using ABAQUS. To achieve this, a concentrated compression load was applied, at intervals. Applying a compressive load would have also yielded accurate results if chosen. A static analysis was then conducted, and the most critical von Mises stress was identified. If this stress exceeded the yield stress, an adjusted load was applied, and the static analysis was iteratively performed until the von Mises stress was equivalent to the yield stress. This iterative process allowed for the determination of the yield strength in the context of the damaged model.

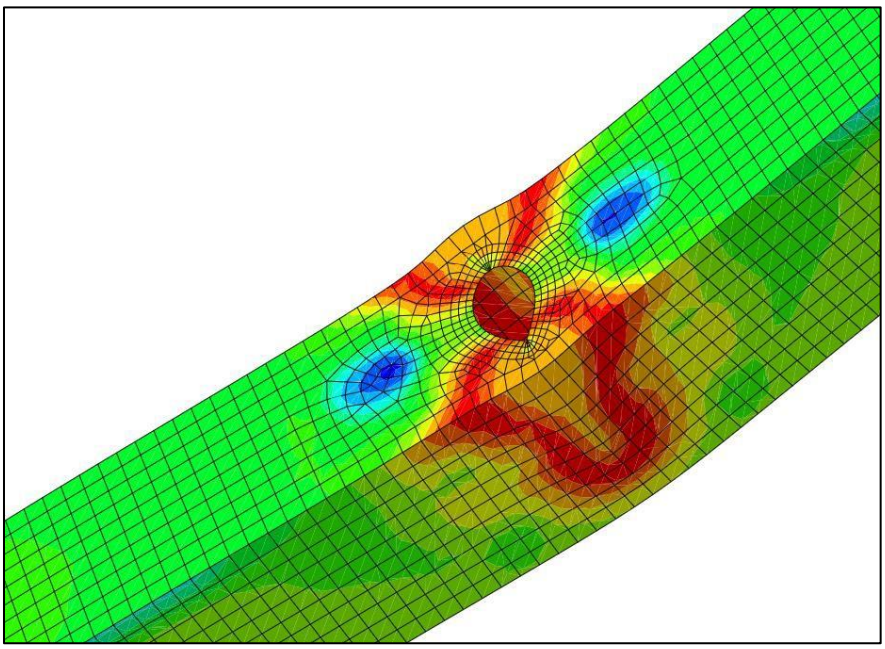

Figure 3-22 von Mises stress in centre damaged member

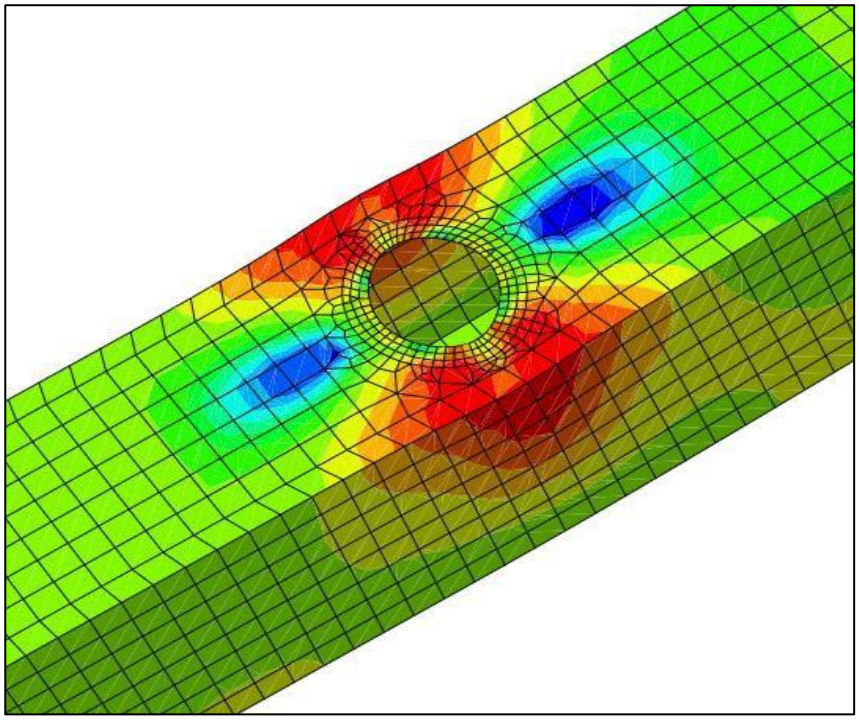

Figure 3-23 von Mises stress in off-centre damage

3.6 Meshing the models

A mesh convergence study was carried out, in accordance with section 3.5.2, to obtain an accurate mesh with no excessive distortions and aspect ratio less than 2. An appropriate mesh, checked via the 'verify mesh' function, is important to ensure accurate results when running the ABAQUS model. S4R elements were selected on ABAQUS to model the hollow sections as thin homogenous shells. The relevance of selecting the S4R elements includes:

- Linear
- Four nodes
- Doubly curved shell element
- Reduced integration
- Hourglass control

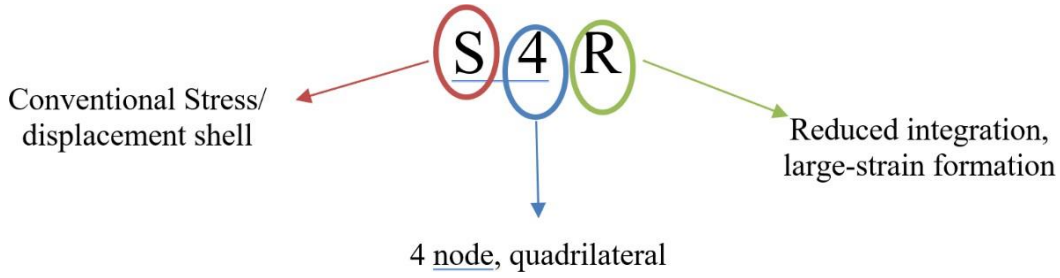

Figure 3-24 Breakdown of S4R

3.7 Determination of Buckling loads

3.7.1 Linear analysis (step 10)

Following the development of the hollow section models in ABAQUS, a linear analysis concerning the buckling behaviour of the models was carried out by selecting the 'buckle' and 'linear perturbation' options in ABAQUS. The buckling load factors were represented as eigenvalues. These eigenvalues were then multiplied by the initially applied load, resulting in the buckling loads corresponding to each eigenvalue. In this model, a load of 1N was applied, ensuring that the eigenvalues and buckling loads were equal. The smallest eigenvalue, in this context, represented the failure load in the linear buckling analysis.

3.7.2 Non-linear analysis (step 11)

For the non-linear analysis of the model, a static Riks analysis was employed in ABAQUS. This type of analysis involves applying small loads in increments. The member will withstand these applied loads until reaching a load high enough to cause buckling. After failure occurs, the applied load starts to decrease. The results are then plotted on a graph, where the x-axis represents load proportionality factors, and the y-axis represents arc length. This graph typically exhibits a general 'n' shape. The load corresponding to each arc length can be determined by multiplying the initial applied loads with the Load Proportionality Factor (LPF). This approach allows for a comprehensive examination of the non-linear behaviour of the model under various loading conditions.

When inputting the actual strain data of the flat and corner specimens, all sets of data were put into the software. The location of the flat and corner specimen regions is indicated in Figure 3-25 below. The flat and corner regions were sized the same as the dog bones.

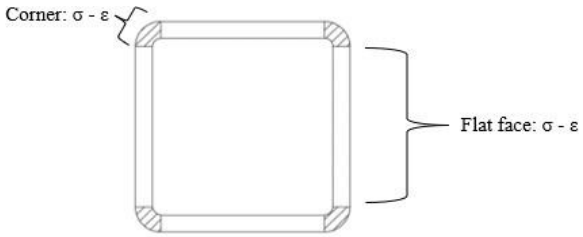

(a) Top View of SHS

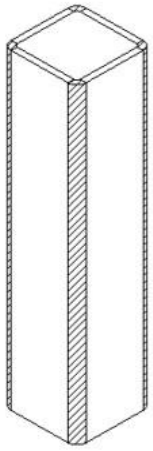

(b) Isometric profile of SHS

Figure 3-25 ABAQUS input of SHS

During manufacturing of the hollow sections, the members underwent shrinkage at different stages due to cutting and welding of the steel. As a result, there was the presence of residual stresses in the member. When comparing the effect of residual stress on slender members, in the literature of (Poursadrollah et al., 2022) and (Chen et al., 2021), it was seen that a member with slenderness less than 0.4 was not significantly impacted by the presence of residual stress as seen in Figure 3-26 below. A slenderness ratio of approximately 0.85 is most impacted by residual stress, thereafter the impact of residual stress on members starts diminishing.

Equation 3-3 for slenderness (defined in the Eurocode) was used to determine whether the tested members fell within the region of 0 – 0.7 (Poursadrollah et al., 2022).

$$\overline{\lambda} = \sqrt{\frac{F_{uy}}{F_{ub}}} \quad \text{..... (3-3)}$$

Where:

$\overline{\lambda}$ equivalent slenderness

F_{uy} yield load

F_{ub} buckling load

Equation 3-3 Equivalent slenderness

The equivalent slenderness for the nine members tested was calculated to be 0.59. According to Figure 3-26, the calculated slenderness value falls within the region of less than 0.7. Therefore, the residual stress is negligible for the tested SHS and does not need to be considered when conducting the non-linear buckling analysis on ABAQUS.

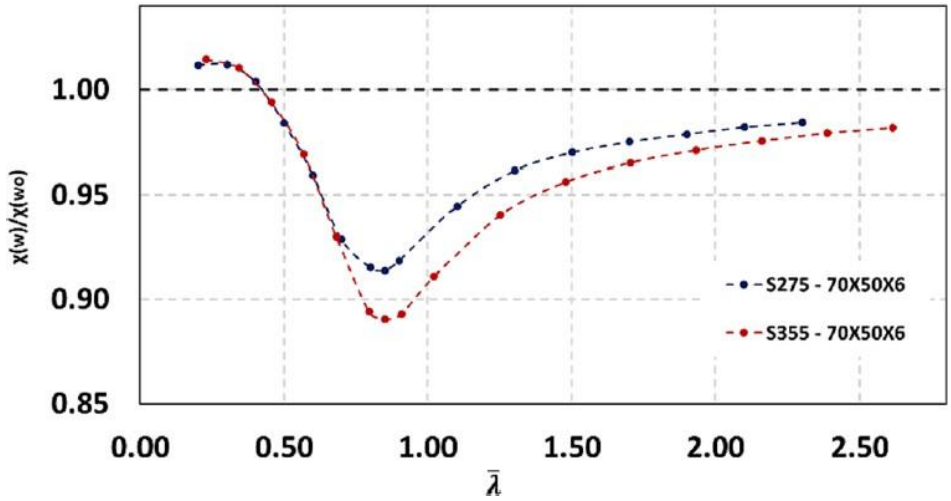

Figure 3-26 Effect of residual stress (Poursadrollah et al., 2022)

3.8 Conclusion of results

Results found via experimental testing in the laboratory and via finite element modelling using the Abaqus software were discussed, tabulated, and graphed.

4. Results and discussion on experimental data and finite element modelling

4.1 Yield strength

4.1.1 Results

The graphical depiction of the effects of damage on a member can be seen in Table 4-1. Both the midway damage and quarter-way damage have been represented. It shows points of peak stress where the material is likely to fail first.

Table 4-1 Modelled behaviour of specimens

Damage	Model	SMises
Undamaged	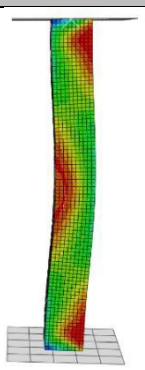	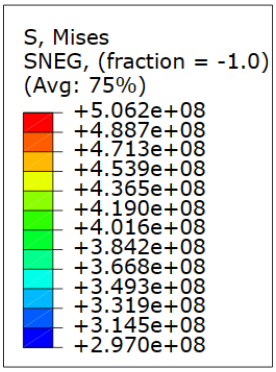
Damaged (Centre hole)	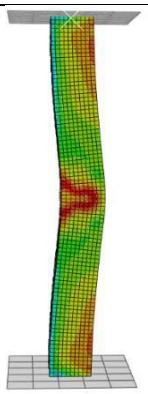	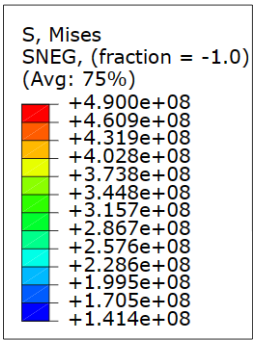
Damaged (Off-centre hole)		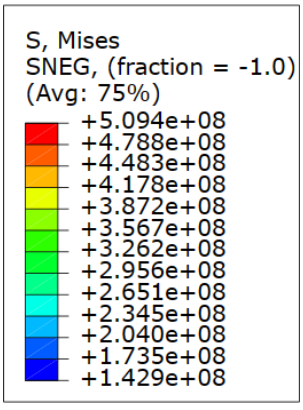

4.1.2 Behaviour of damaged region

The damaged region of the hollow section exhibits an elevated stress concentration. The damage is not confined solely to the specific location of the hole but extends to the sides of the member surrounding the damaged region. This extension results in deformations of the steel, leading to lateral deflections. The lateral deflections are visually evident in Figure 4-1 and Figure 4-2.

Two discernible changes in the steel surrounding the damage can be observed, namely:

- Stretching or warping of the holes
- Thinning of the member steel close to the damaged region

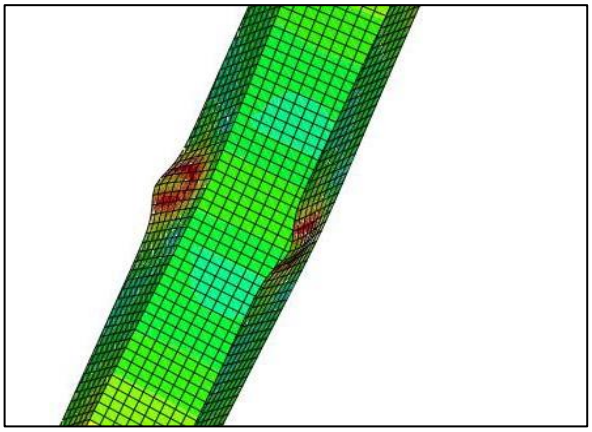

Figure 4-1 Lateral deflections in centre damage - seen form ‘cut’ section

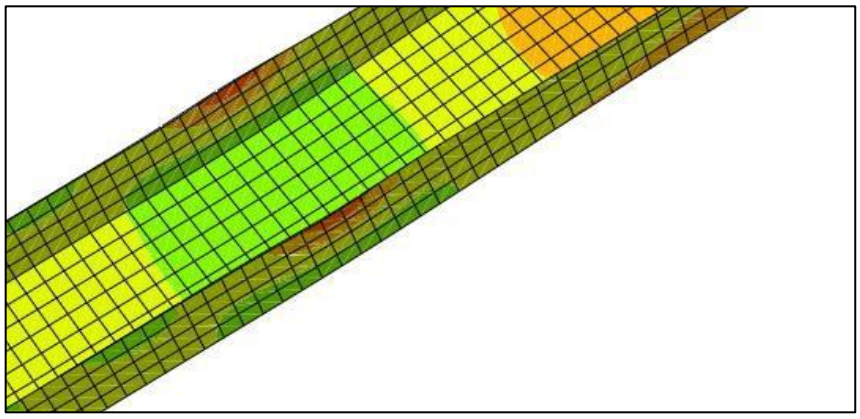

Figure 4-2 Lateral deflection in off-centre damage – seen from ‘cut’ section

4.2 Buckling strength

4.2.1 Results

The buckling strengths of the damaged members were investigated both experimentally and through modelling. Table 4-2 summarises the buckling strengths obtained from the experimental and Table 4-3 summarises the buckling strengths obtained from ABAQUS. The results in these tables are average buckling strengths taken from specimens A, B and C. The

results include the percentage change in strength between damaged and undamaged members. The buckling strengths of the damaged members are consistently lower than those of undamaged members. The impact on the strength is more significant when the damage is at the midspan compared to the quarter-way location. The damaged portion recessed into the member, and the undamaged versus damaged non-linear buckling loads generally a significant portion of their strength.

The observed damage influences the axis of bending, causing a shift where the damage is not on the inside of the specimen. Members failed due to a buckling, characterised by yielding at the corners of the specimen. These results suggest the potential for defining tolerances for acceptable levels of damage in SHS, especially considering critical buckling failure.

Table 4-2 Buckling strength of damaged and undamaged members (based on experimental results)

Undamaged Specimen (Average Group A)	Average buckling strength (kN)	Damaged specimen (centre damage) (Average Group B)	Average buckling strength (kN)	% strength retained after damage
A	327	B	279	85
Undamaged Specimen (Average Group A)	Average buckling strength (kN)	Damaged specimen (off-centre damage) (Average Group C	Average buckling strength (kN)	% strength retained after damage
A	327	C	292	89

Table 4-3 Buckling strength of damaged and undamaged members (based on FEM results)

Undamaged Specimen (Average Group A)	Average buckling strength (kN)	Average buckling strength (kN)	Damaged specimen (centre damage) (Average Group B)	Average buckling strength (kN)	Average buckling strength (kN)	% strength retained after damage	% strength retained after damage
Analysis Type	Linear	Non-linear	Analysis Type	Linear	Non-linear	Linear	Non-linear
A	369.24	310.65	B	328.24	267.84	89	86

Undamaged Specimen (Average Group A)	Average buckling strength (kN)	Average buckling strength (kN)	Damaged specimen (off-centre damage) (Average Group C	Average buckling strength (kN)	Average buckling strength (kN)	% strength retained after damage	% strength retained after damage
Analysis Type	Linear	Non-linear	Analysis Type	Linear	Non-linear	Linear	Non-linear
A	369.24	310.65	C	338.74	271.56	92	87

The percentage of strength retained in experimental testing versus the finite element modelling is comparable. As can be seen in Table 4-2 and Table 4-3, the SHS with a hole at midspan had less strength retained than that of the off-centre hole. When comparing the experimental and finite element strength retained of specimen Bs, experimental testing showed 85% strength retention whereas finite element modelling showed 86% strength retention. When comparing the experimental and finite element strength retained of specimen Cs, experimental testing showed 89% strength retention whereas finite element modelling showed 87% strength retention. There is approximately a 1-2% discrepancy between the experimental results and finite element results making them good representations of one another.

4.2.2 Linear versus non-linear buckling loads

The non-linear buckling loads were lower than the linear buckling loads for the damaged members. In linear analysis, the buckling loads tended to increase with larger member sizes, as observed in the work of Gideon (2021). Consequently, for smaller member sizes, a non-linear analysis may not be deemed necessary as the linear load is not a proportion of the elastic load regardless of size. However, it becomes essential for predicting buckling loads in larger members that experience greater damage. The non-linear analysis provides a more accurate representation of the structural response, particularly in scenarios involving significant damage or larger member sizes where non-linear effects become more pronounced.

5. Comparison study of experimental data and finite element modelling

5.1 Existing literature comparison

Like the findings of Pacheco and Durkin (1988), it can be concluded that hollow sections with damage reduce the buckling strength of the member. However, direct comparison with the study by Pacheco and Durkin (1988) is challenging because their work focused on the impact of dent depth on the yield stress of circular hollow sections, whereas this study investigates the behaviour, both linearly and non-linearly, of SHS due to damage.

There is a scarcity of studies examining the damaged behaviour of SHS. Existing research predominantly concentrates on CHS, particularly in offshore structures, where axial moment, bending moment loading, and lateral loading are relevant, but not applicable to this study. To provide a comprehensive understanding, comparisons were made with linear and non- linear studies on damage-induced imperfections in hollow sections conducted by Elias (2020) and Gideon (2021). Despite variations in hollow section shapes and dent sizes explored in their research, the sections focusing on SHS yielded similar findings to this study regarding the impact of damage on member buckling and member strength.

5.2 Factors which influenced the accuracy of results

5.2.1 Stress concentrations found at member supports

In the stress analysis conducted for the member models, it was observed that stress concentrations occurred at the member supports, as evident in Figure 5-1 and Figure 5-2. Further investigation revealed that these stress concentrations were a consequence of the applied loading and nature of the boundary conditions; and could not be mitigated as they occurred at the supports. However, it was concluded that these stress concentrations did not impact the strength of the member. The high stress at the supports could be caused by the presence of secondary moments from the moments due to member out-of-straightness.

Figure 5-1 Stress concentrations at support (off-centre damage)

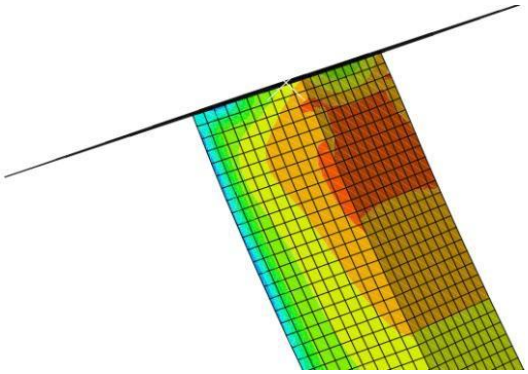

Figure 5-2 Stress concentrations at support (centre damage)

5.2.2 Idealised damage shapes

Section 3.5.4.2 provided a rationale for selecting a hole as the form of damage in the member. While the impact of this damage on the buckling and ultimate strength of the member was explored, research into the effects of varying hole sizes on the members was not conducted. The study focused on the consistent hole size across specimens to maintain uniformity in the experimental and modelling approach. Exploring the influence of different hole sizes is needed for the development of the decision model, offering insights into the variations in structural performance based on the size parameter of the damage.

The idealised damage shape and actual dent shape differs in two aspects. These are explored in Table 5-1.

Table 5-1 Difference between idealised and actual damage

Difference	Reason
Shape of damage	Stress concentrations would be different around dents created due to damage versus ideal created dents. Typically dents have a more ‘diamond’ like shape as opposed to a circle. These sharper edges would cause higher stress concentrations.
Actual damaged material provides restraints to surrounding steel	Provided there no fractures and ultimate strength has not been reached, the material stills experience some restraint even though it has yielded.

Overall, the use of idealised damage was appropriate for the conduction of this study. This will however have decreased the accuracy of the strength and deformations of damaged members.

For ease of modelling, the chosen method of modelling the damage did not consider the plastic material inside the hole which could have impacted the non-linear buckling analysis.

5.2.3 Pattern and size of mesh surrounding the damaged region

During the investigation of the damaged member, it was observed that the member exhibited significant sensitivity to the pattern and mesh size around the damaged region. The mesh size was influenced by mesh curvature, minimum size control values, and global mesh size. The use of minimum size controls and mesh curvature aimed to generate even and symmetric meshes. Undamaged members, in the context of mesh convergence, were not significantly affected by these parameters and, therefore, were not considered during the convergence study.

Given the selection of a constant-sized member, the fineness of the mesh remained consistent across all modelled members. This consistency allows for meaningful comparisons between the results obtained from the damaged and undamaged members.

5.2.4 Limitations on computation time and global mesh size

The global mesh sizes had an impact on the fineness of the mesh and produced results that deviated, greater than or less than, from the theoretical relationships. Accepting the differences between theoretical, model, and practical results was necessitated by the limitations in computational time for each analysis imposed on the study. It is acknowledged that the results would not have been as accurate if a finer global mesh size had been selected, highlighting the trade-off between computational efficiency and result accuracy in the context of the study's constraints.

5.2.5 Conclusion of accuracy of results

The accuracy in results regarding buckling strength and behaviour of the specimens (undamaged and damaged) were compared theoretically, practically and as a modelled member. The accuracy of the study is dependent on:

- Idealised shape of the dent.
- Global mesh size.
- Mesh curvature controls.
- Minimum size controls.

Considering these limitations, the study is still in line with sentiments and conclusions drawn by Pacheco and Durkin (1988), Elias (2020) and Gideon (2021).

5.3 Developing tolerances

The results of this study indicate that damaged members have a significantly lower failure load than that of undamaged members as can be seen in Table 5-2.

Table 5-2 Strength loss of damaged and undamaged members (based on experimental results)

Undamaged Specimen	Average buckling strength (kN)	Damaged specimen (centre damage)	Average buckling strength (kN)	% strength loss after damage
A1	325	B1	274	16
A2	325	B2	281	13
A3	330	B3	282	15
Undamaged Specimen	Average buckling strength (kN)	Damaged specimen (off-centre damage)	Average buckling strength (kN)	% strength loss after damage
A1	325	C1	296	9
A2	325	C2	294	10
A3	330	C3	285	14

Members with central damage experienced a greater loss in strength in comparison to the members with off-centre damage. Gideon (2021) discusses the development of load factors that could be utilised in the industry to calculate buckling loads for damaged members. Rather than discarding members with damage, there may be some tolerance for the use of damaged steel hollow sections.

Table 5-3 and Table 5-4 depict the force that a member can be withstood before failure by comparing the strength loss due to various hole sizes. A decision model would need to provide suitable tolerances on how to approach damaged members and using them in industry. A larger and more comprehensive study encompassing a broader range of hollow sections and varying sizes and locations of damage would be necessary to further validate and generalise these findings. With the incorporation of a factor of safety, the results from this study could potentially be implemented in the industry.

5.4 Effect on member strength due to varying levels of damage

The experimental testing involved testing of 3 undamaged, 3 centre damage and 3 off-centre damage specimens. The damaged specimens had a circular hole size diameter of 25mm. To assess the impact of varying levels of damage on strength loss, the following hole sizes were used in the ABAQUS software- 5mm, 15mm, 25mm and 35mm.

Table 5-3 and Table 5-4 depicts the ABAQUS results of strength loss in damaged members with varying hole sizes.

Table 5-3 Effects on strength loss due to varying hole sizes (centre hole)

Specimen size (mm) b x l x t	Length (mm)	Hole size (mm)	Cross sectional area (mm^2)	Yield stress (MPa)	Effective area (mm^2)	Force (kN)
50x50x4	450	5	384	492	364	179
50x50x4	450	15	384	497	324	161
50x50x4	450	25	384	491	284	139
50x50x4	450	35	384	502	244	122

Where:

Effective Area = Cross sectional area – (hole x thickness)
Force = Yield stress x effective area

Table 5-4 Effects on strength loss due to varying hole sizes (off-centre hole)

Specimen size (mm)	Length (mm)	Hole size (mm)	Cross sectional area (mm2)	Yield stress	Effective area	Force (kN)
50x50x4	450	5	384	474	364	172.536
50x50x4	450	15	384	483	324	156.492
50x50x4	450	25	384	509	284	144.556
50x50x4	450	35	384	502	244	122.488

As the hole becomes larger in diameter, the failure load/force becomes smaller. Table 7-3 depict the 5mm and 35mm hole for the damaged specimens.

Table 5-5 Modelled damaged members with varying hole sizes

Damaged member	Dent size (mm)	Modelled member
Centre	5	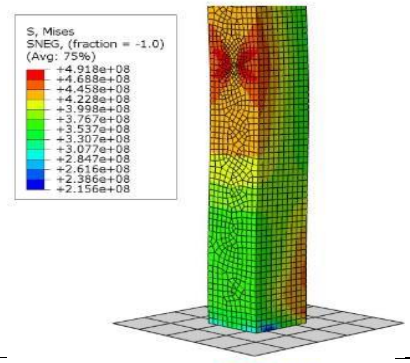
Centre	35	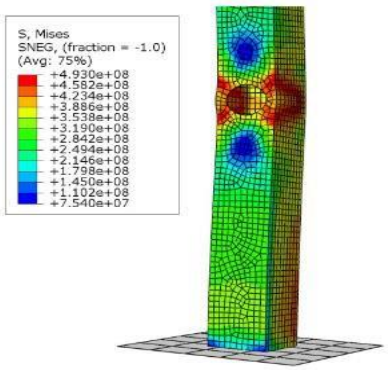
Off-centre	5	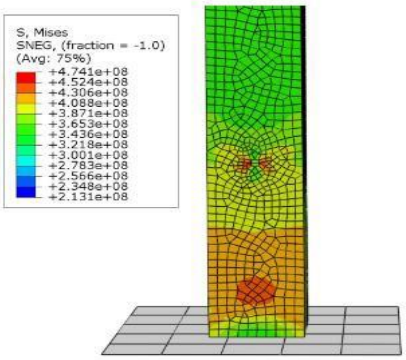
Off-centre	35	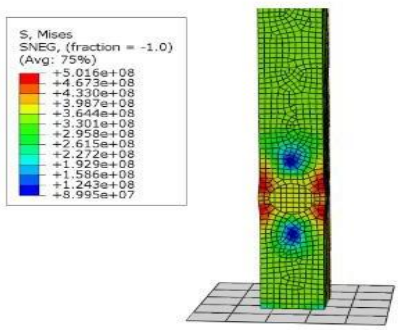

5.5 Decision model

The formulation of a comprehensive decision model for handling damaged members is required. This model will provide a systematic framework for determining the appropriate action for damaged SHS members by making use of a utilisation model and zoning.

5.5.1 Utilisation model

When determining whether the damaged hollow section falls within Zone 1 (keep member) or Zone 2 (replace or repair member), calculations need to be carried out.

C_u – applied load on member

C_r – load at failure on a member

$C_r = (\phi A f_y (1 + \lambda 2n))^{\frac{-1}{n}}$

For the member to still be used in construction (kept), it needs to fall in Zone 1. The $C_r > C_u$.
After damage, $C_r \rightarrow C_{r2}$

Therefore, $\frac{C_u}{C_r} \leq 1$. The damaged member is then okay to be used in application.

The C_u, in the member, comes from the analysis and is compared to C_{r1} (in the undamaged member). After damage, C_{r2} is found. If the, $\frac{C_u}{C_{r2}} \leq 1$, then the member will be kept.

5.5.2 Zones

The graph in Figure 5-3 has been divided into two zones, namely:

Zone 1: Keep (based on utilisation ratio) – $\frac{C_u}{C_{r2}}$

Zone 2: Repair/Replace (based on utilisation ratio)

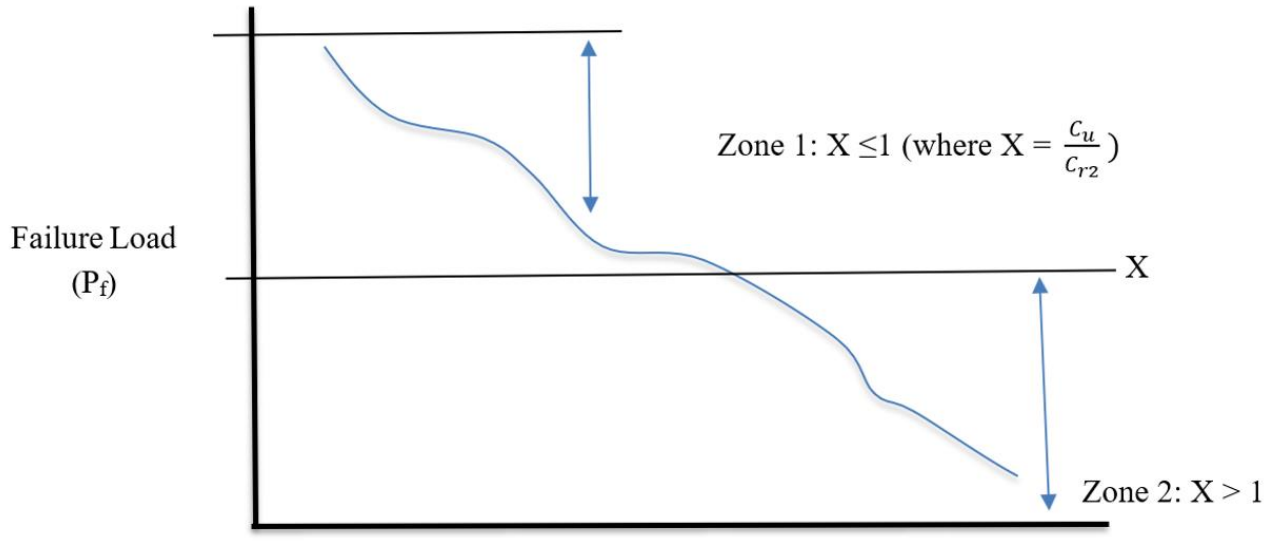

Figure 5-3 Zones for a damaged SHS section

Example calculation for hypothetical member:

Cu = 260 kN

Safety factor = 1.15

$C_r = \frac{325}{1.15} = 282.61$, where $C_r = \frac{C_{exp}}{\gamma_m}$

$\frac{Cu}{Cr} = \frac{260}{282.61} = 0.92$ (keep)

Example calculation for hypothetical member:

Cu = 245kN

Safety factor = 1.15

$Cr = \frac{274}{1.15} = 238.26$

$\frac{C_u}{C_r} = \frac{245}{238.26} = 1.03$ (replace)

6. Conclusion and Recommendations

6.1 Conclusion

In the investigation of the behaviour of SHS subjected to damage, practical laboratory testing and FEM using ABAQUS were conducted. To maintain consistency in evaluating the effects of damage on commercially available members, nine samples of equal sizes were utilised—three undamaged, three damaged with a midspan hole, and three damaged with a quarter-way hole. Stress analysis, linear, and non-linear analyses were performed.

Analysis of the experimental data and finite element models revealed that damaged members experienced lower buckling strengths due to localised stress concentrations around the damaged region. Larger holes caused deformation around the edges of the damaged regions and induced lateral deflections during yielding. Despite limitations related to the idealised hole size, global mesh size, minimum size control values, and mesh curvature, the results largely agreed with previous studies. The reduction in buckling strength for damaged members was found to not be significantly different to that of undamaged members.

This study considered Euler's formula, laboratory tests, and linear and non-linear buckling strengths. Overall, it determined that the buckling strength is significantly reduced in damaged members, warranting the consideration of developing tolerances for imperfections, particularly for members subjected to failure. Strength loss is higher (approximately 15%) for a hole at midspan as opposed to strength loss for a hole at off -centre (approximately 11%). There may be potential for developing tolerances for members subjected to buckling failure if a decision model is used to determine whether a damaged member is suitable to use in industry. The larger the size of the damage, the less strength retained in the member. The failure of damaged members can be predicted and thereafter compared to the prescribed zoning conditions in the decision model to determine the suitability and utilisation of the damaged member.

The study aligns with current practices specified in SANS Code 2001-CS1(2005), which requires the repair of damaged hollow sections to their existing tolerances for manufacturing. The evidence provided in this investigation supports and reinforces these current repair practices whilst also providing tolerances for the utilisation of damaged members by use of the decision model.

6.2 Recommendations

The results of this study support the continued use of the current practices regarding the repair of damaged SHS as stated in the SANS Code 2001-CS1(2005) whilst also providing a decision model to determine a utilisation factor for damaged members. However, the following is suggested regarding further study:

- Use of a wider range of specimen sizes will allow for a more holistic overview of the effects of the damage and a parametric study if the FEM model is accurate enough.
- More accurate dent shapes to be developed from research into literature or testing in the laboratory.
- Testing of other damage profiles on members as opposed to only flat face damage.
- In damaged areas, the mesh should be refined.

References

- Alithari, A.S. 2014. Shape of fatigue failure of steel shaft. [3]. | *download scientific diagram, ResearchGate*. Available: https://www.researchgate.net/figure/Shape-of-Fatigue-Failure-of-Steel-Shaft-3_fig1_267632191 [2024, September 01]
- Apostolopoulos, C. & Koulouris, K. 2021. Corrosion Effect on Bond Loss between Steel and Concrete. In *Structural Integrity and Failure*. R. Oyguc & F. Tahmasebinia, Eds. DOI: 10.5772/intechopen.94166.
- Cerik, B.C. 2015. Ultimate strength of locally damaged steel stiffened cylinders under axial compression. *Thin-Walled Structures*. 95:138–151. DOI: 10.1016/j.tws.2015.07.004.

- Chen, J., Fang, H. & Chan, T.M. 2021. Design of fixed-ended octagonal shaped steel hollow sections in compression. *Engineering Structures*. 228. DOI: 10.1016/j.engstruct.2020.111520.

- Cho, S., Kwon, J. & Kwak, D. 2010. Structural Characteristics of Damaged Offshore Tubular Members. *Journal of Ocean Engineering and Technology*. 24(4):1–7.
- Comité International pour le Développement et l´Etude de la Construction Tubulaire. n.d. Welcome to CIDECT. Available: https://www.cidect.org/ [2023, September 3].
- Dubinskii, S., Feygenbaum, Y., Senik, V. & Metelkin, E. 2019. A study of accidental impact scenarios for composite wing damage tolerance evaluation. *Aeronautical Journal*. 123(1268):1724–1739. DOI: 10.1017/aer.2018.152.

  Durkin, S. 1987. An Analytical Method for Predicting the Ultimate Capacity of a Dented Tubular Member. *International Journal of Mechanical Sciences.* 29(7):449-467.

- Dutta, D., Wardenier, J., Yeomans, N., Sakae, K., Bucak, Ö. & Packer, J.A. 1998. Design Guide for Fabrication, Assembly and Erection of Hollow Section Structures. *CIDECT*. Available: https://www.cidect.org/design-guides/ [2023, August 8].
- Dzioba, I., & Lipiec, S. 2018. Calibration of the constitutive equations for materials with different levels of strength and plasticity characteristic based on the uniaxial tensile test data. *IOP Conference Series: Materials Science and Engineering*, *461*(1), 0– 6.https://doi.org/10.1088/1757-899X/461/1/012018
- Elias, N. 2020. Investigation into the Effects of Damage-Induced Imperfections on Steel Hollow Section Truss Members (Issue December). University of Cape Town.
- Ellinas, C.P. 1984. Ultimate Strength of Damaged Tubular Bracing Members. *Journal of Structural Engineering*. 110(2):245–259. DOI: 10.1061/(asce)0733-9445(1984)110:2(245).

- Ellobody, E., Feng, R. & Young, B. 2013. *Finite Element Analysis and Design of Metal Structures*. Butterworth-Heinemann. DOI: 10.1016/C2012-0-07230-4.

- Foster, A.S.J., Gardner, L. & Wang, Y. 2015. Practical strain-hardening material properties for use in deformation-based structural steel design. *Thin-Walled Structures*. 92:115–129. DOI: 10.1016/j.tws.2015.02.002.

- Gardner, L., Saari, N., & Wang, F. 2010. Comparative experimental study of hot-rolled andcold-formed rectangular hollow sections. *Thin-Walled Structures*, *48*(7), 495–507. https://doi.org/10.1016/j.tws.2010.02.003
- Godoy, L. A. 1st Ed. 1996. Thin-Walled Structures with Structural Imperfections. Oxford, UK: Pergamon. Available: Google Books [2023, September 3].
- Gideon, K. 2021. Nonlinear analysis of Hollow Structural Sections (HSS) members with damage-o=induced imperfections. University of Cape Town.
- Harper, W.J. 1976. The Use of Steel in Bridge Construction. Philosophical Transactions of the Royal Society of London. Series A, Mathematical and Physical Sciences. 282(1307): 37-40. Available: https://www.jstor.org/stable/74521 [2023, September 3].
- Ibrahim, A. M., & Khalaf, M. S. 2018. Elastic-plastic behavior of circular hollow section steel tubes subjected to bending. *Journal of Engineering Science and Technology Review*, *11*(3), 42–49.https://doi.org/10.25103/jestr.113.06
- Iman, M., Suhendro, B., Priyosulistyo, H. & Muslikh. 2018. Numerical Investigation on the Buckling Failure of Slender Tubular Member with Cutout Presence. *Applied Mechanics and Materials*. 881:122–131. DOI: 10.4028/www.scientific.net/amm.881.122.

- Kachanov, L.M. 1986. *Introduction to Continuum Damage Mechanics*. 1st ed. V. 54. Springer Dordrecht. DOI: https://doi.org/10.1007/978-94-017-1957-5.

- Lau, H.H., Shek, P.N., Ahmad Kueh, B.H. & Mahmood, M.T. 2014. Economic aspect of square hollow section in the design of multi-storey unbraced steel frame. *Materials Research Innovations*. 18:164–168. DOI: 10.1179/1432891714Z.000000000951.

- Lim, H., & Hoag,S.W. 2013. Plasticizer Effects on Physical–Mechanical Properties of Solvent Cast Soluplus® Films. Available: https://www.researchgate.net/publication/236924185_Plasticizer_Effects_on_Physical-Mechanical_Properties_of_Solvent_Cast_SoluplusR_Films[2023,September 5]
- Mansur, A. 2011. MODELING OF MECHANICAL PROPERTIES OF CERAMIC- METAL COMPOSITES FOR ARMOR APPLICATIONS. (September). Available:https://www.researchgate.net/publication/267254926_MODELING_OF_MECHANICAL_PROPERTIES_OF_CERAMIC- METAL_COMPOSITES_FOR_ARMOR_APPLICATIONS [2023, September 08].
- Moore, P. & Booth, G. 2015. Brittle fracture and the behaviour of cracks in structures. In *The Welding Engineers Guide to Fracture and Fatigue*. 45–63. DOI: 10.1533/9781782423911.1.45.
- Mirambell, E. 2004. Structural damage in steel construction: regulatory aspects. *Progress in Structural Engineering and Materials*. 6(1):56-68. DOI: 10.1002/pse.165.
- Mordini, F. 2014. Structural Hollow Sections – From an Engineer's Perspective. *Steel Construction Journal*. 38(3):40-42.77.
- Mudenda, K. 2008. Performance of Cold Formed Welded Tubular Steel Joints under Moment Loading. M.Sc. Thesis. University of Cape Town.
- Narendra, P.V.R. & Singh, K.D. 2016. Structural performance of elliptical hollow section (EHS) steel

tubular braces under extremely low cycle fatigue loading - a finite element study. *Thin-Walled Structures*. 109:202-216. DOI: 10.1016/j.tws.2016.09.025

- Pacheco, L.A. & Durkin, S. 1988. Denting and collapse of tubular members-A numerical and experimental study. *International Journal of Mechanical Sciences*. 30(5):317–331. DOI: 10.1016/0020-7403(88)90104-X.
- Padula, J. A., & Ostapenko, A. (1988). Indentation Behavior of Tubular Members (No. 508.8) (Issue 38).
- Parrott, G. 2014. Structural Steel Design to SANS 10162:1-2005. Durban, South Africa: SHADES Technical Publications.
- Petrusma, J., Ghanbari-Ghazijahani, T. & Jiao, H. 2021. Buckling of steel cylindrical hollow sections with large imperfections under compression. *Proceedings of the Institution of Civil Engineers: Structures and Buildings*. 174(3):159–168. DOI: 10.1680/jstbu.17.00181.

- Poursadrollah, A., D'Aniello, M. & Landolfo, R. 2022. Experimental and numerical tests of cold-formed square and rectangular hollow columns. *Engineering Structures*. 273. DOI: 10.1016/j.engstruct.2022.115095.

- Prabu, B., Raviprakash, A. V. & Venkatraman, A. 2010. Parametric study on buckling behaviour of dented short carbon steel cylindrical shell subjected to uniform axial compression. *Thin-Walled Structures*. 48(8):639–649. DOI: 10.1016/j.tws.2010.02.009.
- Priya C, B., Keerthana, M., Verma, M. & Banjara, N. 2011. Design of steel channel tension members-proposal to IS 800:2007. *Journal of Structural Engineering (Madras)*. 38:122–130.Available:https://www.researchgate.net/publication/285518380_Design_of_steel_channel_tension_members-proposal_to_IS_8002007 [2023, September 08].
- Roylance, D. 2001. Stress-Strain Curves [Lecture notes]. Department of Materials Science and Engineering, Massachusetts Institute of Technology.
- South African National Standards. 2012. Construction works: part CS1: Structural steelwork. (SANS 2001-CS1:2012). Pretoria: SANS.
- Southern African Institute of Steel Construction. 2016. Southern African Steel Construction Handbook. 8th ed. Johannesburg, South Africa: Southern African Institute of Steel Construction.
- Šmak, M. & Straka, B. 2012. Geometrical and structural imperfections of steel member systems. In *Procedia Engineering*. V. 40. 434–439. DOI: 10.1016/j.proeng.2012.07.121.
- South African National Standard. (2005). Construction works Part CS1: Structural steelwork (Ed.1). Standards South Africa.
- Tan, Z.H., Liu, L.S., Sun, Y.S. & Cho, C. 2015. Response of an Indented Square Tube Under Impact Loading. *Strength of Materials*. 47(1):156–163. DOI: 10.1007/s11223-015-9642-2.
- The Heritage Portal. 2016. A Short History of Steel. Available: http://www.theheritageportal.co.za/article/short-history-steel [2023, July 3].
- Wardenier, J. 2001. *Hollow Sections in Structural Applications*. *CIDECT*. Available: https://www.cidect.org/books/ [2023, July 3]
- Wardenier, J., Packer, J., Zhao, X., & van der Vegte, G. 2010. Hollow Sections in Structural Applications (2nd Ed.). CIDECT. Available: https://www.cidect.org/books/[2023, September 5]

- Wu, Y., Jin, P. & Zhang, P. 2017. Theoretical analysis of pipeline with type I dent under the external force. *Advances in Mechanical Engineering*. 9(5). DOI: 10.1177/1687814017705599.
- Zhao, X.L., Wilkinson, T. & Hancock, G. 2005. *Cold-formed tubular members and connections: Structural behaviour and design*. DOI: 10.1016/B978-0-08-044101-6.X5000-2.

Appendix

SPECIMEN TYPE	QUANTITY
UNDAMAGED	3
OFF-CENTER DAMAGE	3
CENTER DAMAGE	3

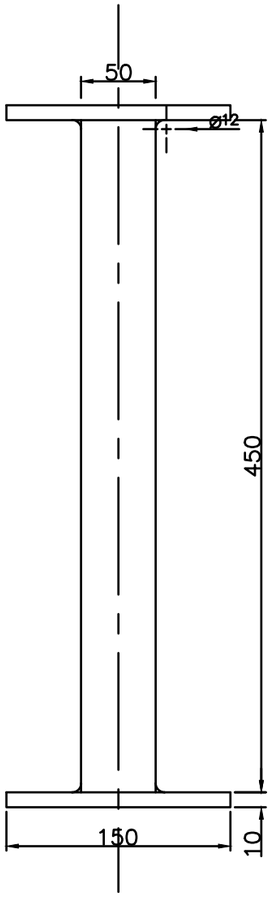

TYPE A
UNDAMAGED STEEL
HOLLOW SECTION X3

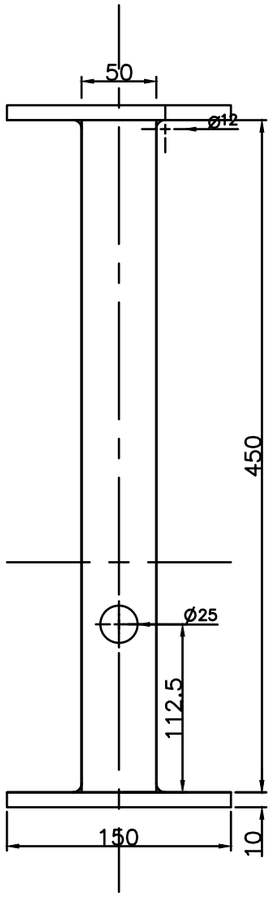

TYPE B
OFF-CENTER DAMAGED STEEL
HOLLOW SECTION X3

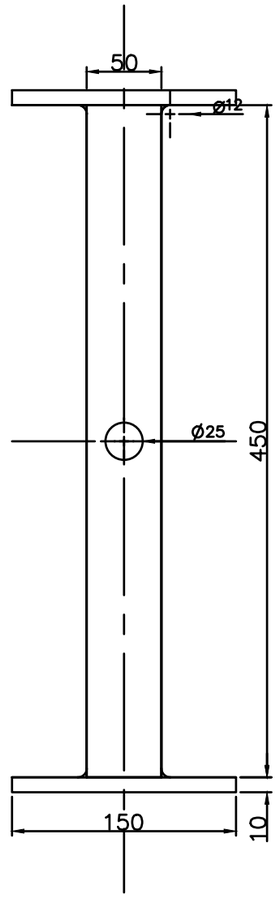

TYPE C
CENTER DAMAGED STEEL
HOLLOW SECTION X3

Notes:

NOTES:
ALL DIMENSIONS ARE IN MILLIMETERS (mm)

REV:	DESCRIPTION:	BY:	DATE:

STATUS:

CIVIL ENGINEERING
NEB, MADIBA CIRCLE
UPPER CAMPUS, RONDEBOSCH
Telephone +27 (0) 21 650 2584
www.civil.uct.ac.za

CLIENT:

ARCHITECT:

SITE:

TITLE:

SCALE AT A3:	DATE:	DRAWN:	CHECKED:
1:4			
PROJECT NO:	DRAWING NO:		REVISION:

Appendix A2: Dog bone drawings

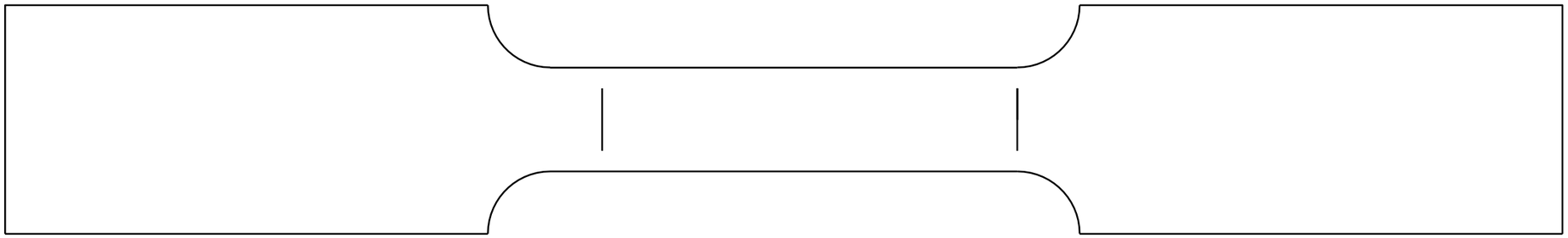

TENSILE TEST SPECIMEN (STEEL)

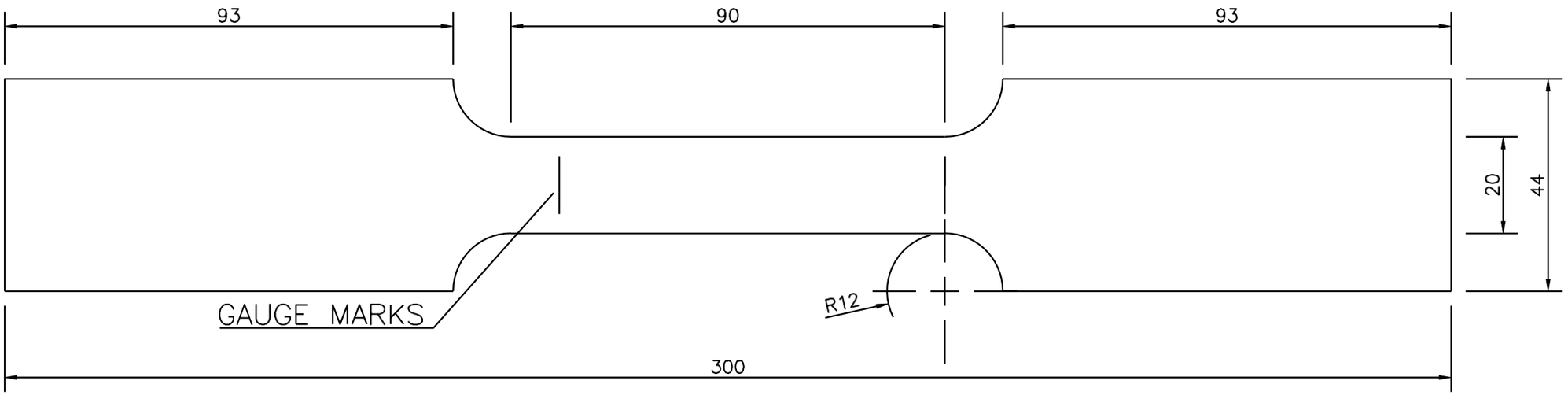

4No. SPECIMENS FROM SHS SIDE FACE

Tolerance (L_0) = +-0.1mm

Notes:

NOTES:
ALL DIMENSIONS ARE IN MILLIMETERS (mm)

SHS STEEL HOLLOW SECTION

REV:	DESCRIPTION:	BY:	DATE:

STATUS:

CIVIL ENGINEERING
NEB, MADIBA CIRCLE
UPPER CAMPUS, RONDEBOSCH
Telephone +27 (0) 21 650 2584
www.civil.uct.ac.za

CLIENT: N/A

ARCHITECT: B. Larknath

SITE: N/A

TITLE: Dog bone drawings

SCALE AT A3:	DATE:	DRAWN:	CHECKED:
1:1	9/09	BL	
PROJECT NO:	DRAWING NO:		REVISION:

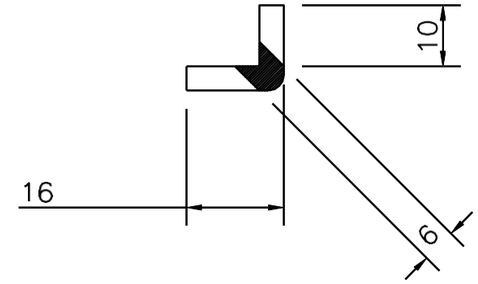

SECTION

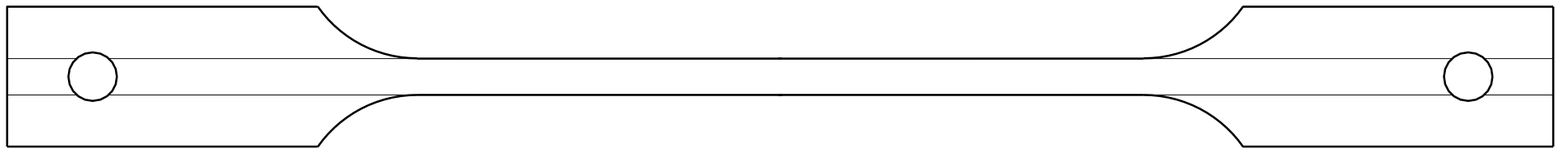

SHS CORNER SPECIMEN

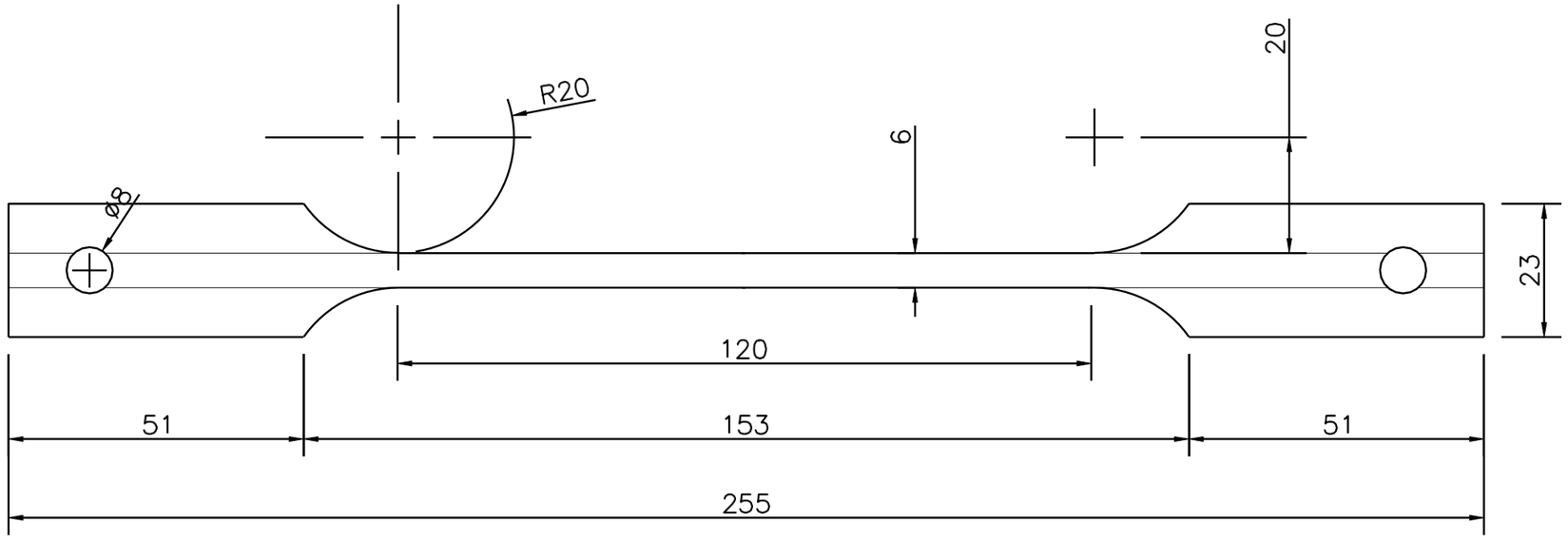

4No. SPECIMENS FROM SHS SIDE FACE

Tolerance (L_0) = +-0.1mm

Notes:

NOTES:
ALL DIMENSIONS ARE IN MILLIMETERS (mm)
SHS STEEL HOLLOW SECTION

REV:	DESCRIPTION:	BY:	DATE:

STATUS:

CIVIL ENGINEERING
NEB, MADIBA CIRCLE
UPPER CAMPUS, RONDEBOSCH
Telephone +27 (0) 21 650 2584
www.civil.uct.ac.za

CLIENT: N/A

ARCHITECT: B.Larknath

SITE: N/A

TITLE: Dog bone drawings

SCALE AT A3:	DATE:	DRAWN:	CHECKED:
1:1	9/09	BL	

PROJECT NO:	DRAWING NO:	REVISION:

Appendix B: Out-of-straightness readings

Member State	Member Damage	Member Name	Measurements x-x	Out-of-Straightness readings x-x	Out-of-Straightness readings y-y
Undamaged	Undamaged	A1	50	0	0
			100	+0.01	-0.03
			150	-0.02	-0.01
			200	-0.02	+0.03
			250	-0.02	+0.03
			300	-0.01	+0.01
			350	0	0
		A2	50	0	0
			100	-0.04	+0.01
			150	-0.03	+0.02
			200	-0.03	+0.02
			250	-0.03	+0.02
			300	-0.03	-0.01
			350	0	0
		A3	50	0	0
			100	-0.01	-0.03
			150	-0.03	-0.04

			200	-0.03	-0.04
			250	-0.04	-0.03
			300	-002	-0.03
			350	0	0
Damaged	Damaged Centre Hole	B1	50	0	0
			100	+0.01	-0.01
			150	+0.03	-0.01
			200	+0.03	-0.02
			250	+0.01	-0.03
			300	0	-0.02
			350	0	0
		B2	50	0	0
			100	-0.02	-0.04
			150	-0.03	-0.03
			200	-0.03	-0.03
			250	-0.02	-0.01
			300	-0.01	-0.01
			350	0	0
		B3	50	0	0
			100	-0.01	0

			150	-0.02	-0.01
			200	-0.03	-0.01
			250	-0.01	-0.01
			300	-0.01	-0.02
			350	0	0
	Damaged Off-centre hole	C1	50	0	0
			100	-0.02	+0.02
			150	-0.04	0
			200	-0.03	-0.01
			250	-0.03	-0.02
			300	-0.01	-0.01
			350	0	0
		C2	50	0	0
			100	+0.02	0
			150	0	0
			200	-0.01	0
			250	-0.02	-0.01
			300	+0.01	-0.01
			350	0	0
		C3	50	0	0

			100	+0.02	+0.02
			150	+0.02	0
			200	-0.01	-0.01
			250	-0.02	-0.02
			300	-0.01	-0.01
			350	0	0

Appendix C: Load-Displacement Graphs and readings

A1

Force (kN)	Displacement (mm)
0	0
10	0
20	0
30	0
40	0
50	0
60	0
70	0
80	0
90	0
100	0
110	0
120	0
130	0
140	0
150	0
160	0
170	0
180	0
190	0
200	0
210	0
220	0
230	0
240	0
250	0
260	0
270	0
280	0
290	0,004
300	0,228
310	1,627
320	12,673
325	13,211

A2

Force (kN)	Displacement (mm)
0	0
10	0
20	0
30	0
40	0
50	0
60	0
70	0
80	0
90	0
100	0
110	0
120	0
130	0
140	0
150	0
160	0
170	0
180	0
190	0
200	0
210	0
220	0
230	0
240	0
250	0
260	0
270	0
280	0,008
290	0,557
300	2,609
310	4,428
320	11,372
325	13,509

A3

Force (kN)	Displacement (mm)
0	0
10	0
20	0
30	0
40	0
50	0
60	0
70	0
80	0
90	0
100	0
110	0
120	0
130	0
140	0
150	0
160	0
170	0
180	0
190	0
200	0
210	0
220	0
230	0
240	0
250	0
260	0
270	0
280	0
290	0
300	0
310	0,145
320	6,659
325	8,011

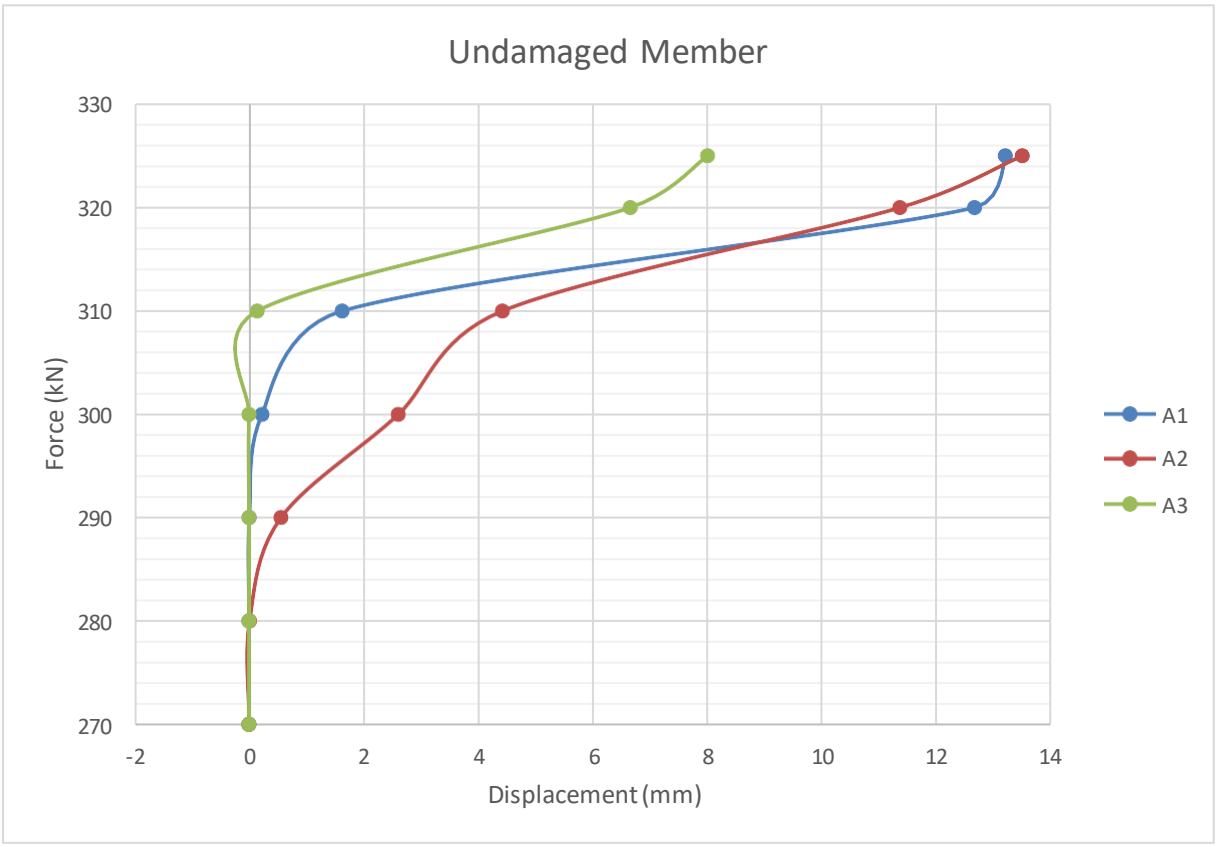
Undamaged Member
330
320
310
300
290
280
270
Force (kN)
-2
0
2
4
6
8
10
12
14
Displacement (mm)
A1
A2
A3

B1

Force (kN)	Displacement (mm)
0	0
10	0
20	0
30	0
40	-0,027
50	-0,027
60	-0,027
70	-0,027
80	-0,027
90	-0,027
100	-0,027
110	-0,022
120	-0,021
130	-0,019
140	-0,004
150	0,029
160	0,059
170	0,095
180	0,128
190	0,183
200	0,21
210	0,294
220	0,342
230	0,445
240	0,609
250	0,855
260	1,168
270	3,345
274	9,963

B2

Force (kN)	Displacement (mm)
0	0
10	-0,016
20	-0,021
30	-0,021
40	-0,021
50	-0,021
60	-0,021
70	-0,021
80	-0,021
90	-0,021
100	-0,021
110	-0,021
120	-0,021
130	-0,021
140	-0,021
150	-0,021
160	-0,021
170	-0,021
180	-0,021
190	-0,021
200	-0,021
210	-0,01
220	0,184
230	0,365
240	1,689
250	2,437
260	3,334
270	4,458
280	5,137
282	5,529

B3

Force (kN)	Displacement (mm)
0	0
10	-0,058
20	-0,063
30	-0,071
40	-0,071
50	-0,071
60	-0,071
70	-0,071
80	-0,071
90	-0,075
100	-0,084
110	-0,088
120	-0,095
130	-0,095
140	-0,095
150	-0,095
160	-0,095
170	-0,095
180	-0,095
190	-0,095
200	-0,095
210	-0,095
220	-0,087
230	-0,07
240	-0,01
250	0,097
260	0,294
270	0,778
280	2,035
282	6,892

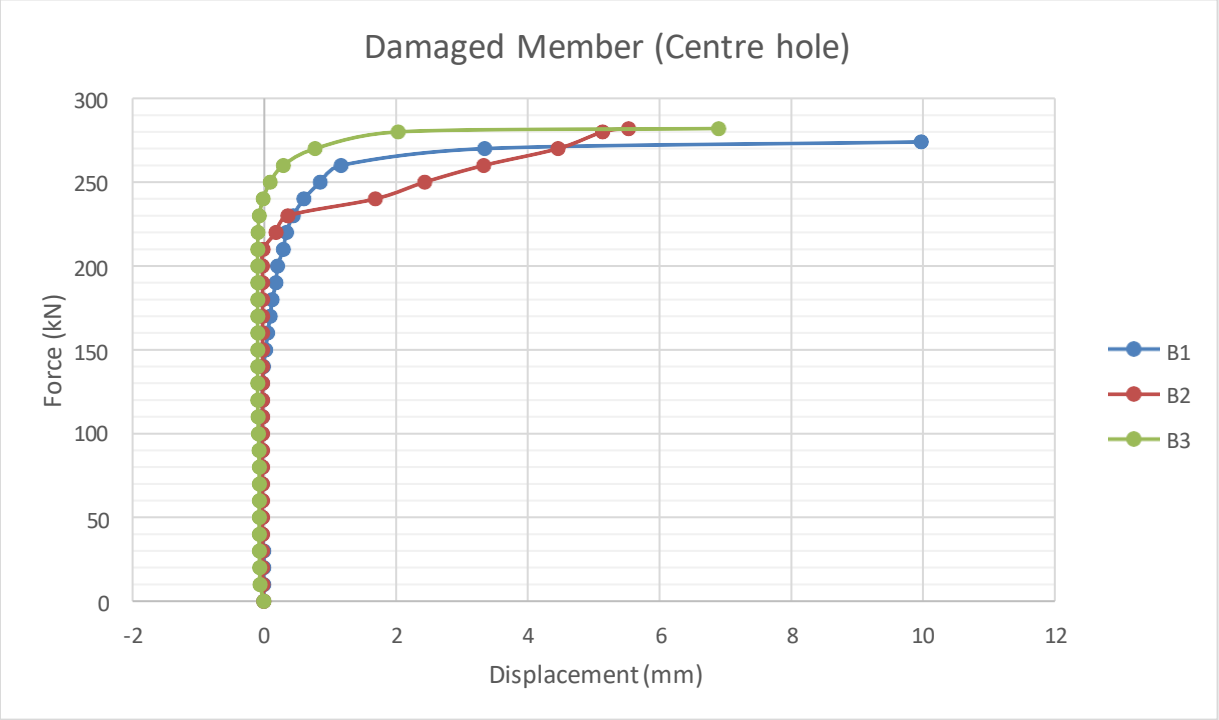

C1

Force (kN)	Displacement (mm)
0	0
10	0
20	0
30	0
40	0
50	0
60	-0,005
70	-0,009
80	-0,01
90	-0,012
100	-0,018
110	-0,024
120	-0,028
130	-0,035
140	-0,039
150	-0,043
160	-0,044
170	-0,048
180	-0,048
190	-0,048
200	-0,048
210	-0,048
220	-0,048
230	-0,048
240	-0,048
250	-0,033
260	0,014
270	0,073
280	1,146
290	3,592
296	5,436

C2

Force (kN)	Displacement (mm)
0	0
10	-0,025
20	-0,025
30	-0,025
40	-0,025
50	-0,025
60	-0,025
70	-0,025
80	-0,025
90	-0,025
100	-0,025
110	-0,025
120	-0,025
130	-0,025
140	-0,025
150	-0,025
160	-0,053
170	-0,073
180	-0,096
190	-0,096
200	-0,096
210	-0,096
220	-0,096
230	-0,096
240	-0,063
250	0,059
260	1,003
270	1,674
280	2,115
290	4,012
294	5,343

C3

Force (kN)	Displacement (mm)
0	0
10	-0,001
20	-0,001
30	-0,001
40	-0,001
50	-0,001
60	-0,001
70	-0,001
80	-0,001
90	-0,001
100	-0,001
110	-0,001
120	-0,001
130	-0,001
140	-0,001
150	-0,001
160	-0,001
170	-0,001
180	-0,001
190	-0,001
200	-0,001
210	-0,001
220	-0,001
230	-0,001
240	-0,001
250	0,007
260	0,037
270	0,275
280	1,034
290	5,259
294	5,259

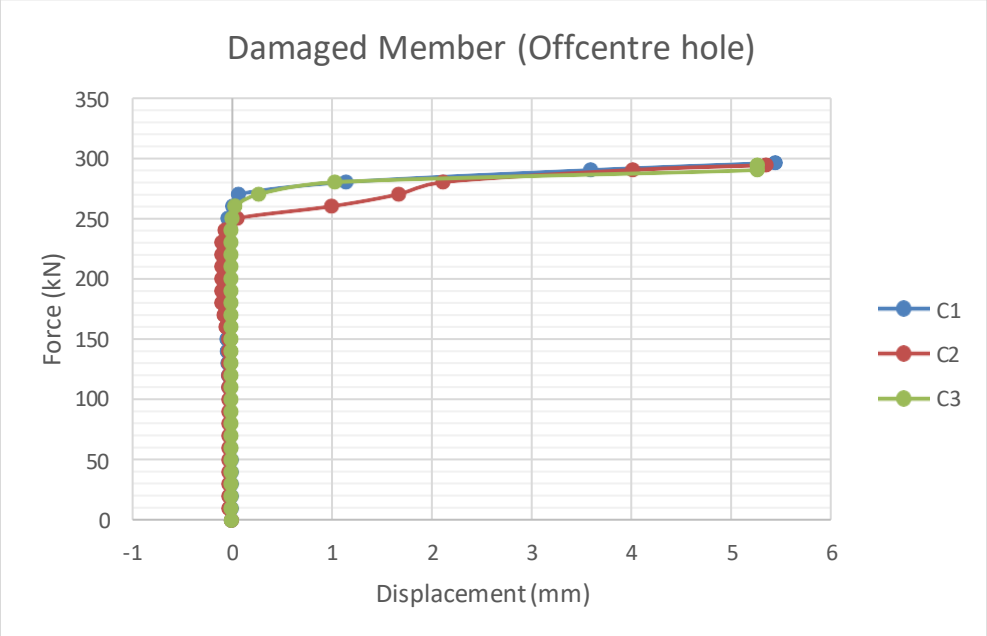

Appendix D: Tensile Testing Results

	Force (N)	Area (mm^2)	Original length	Elongation	Final length	Stress	Strain
Flat 1	34413,10156	83,4768	94,2	13,96	108,16	412247493	0,1482
Flat 2	34903,90625	83,9108	92,52	9,49	102,01	415964408	0,10257
Flat 3	33845,39844	81,891	91,72	13,99	105,71	413298146	0,15253
Corner 1	14798,53613	30	125,72	5,38	131,1	493284538	0,04279
Corner 2	15391,21973	30	125,41	7,61	133,02	513040658	0,06068
Corner 3	14424,23438	30	126,59	7,47	134,06	480807813	0,05901

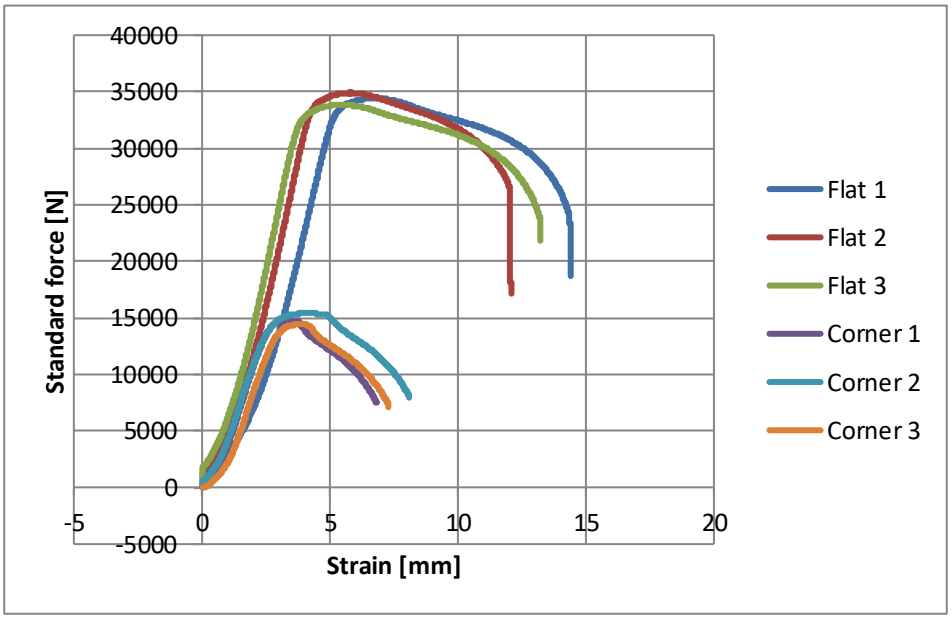

Appendix E: Job Safety

UNIVERSITY OF CAPE TOWN
DEPARTMENT OF CIVIL ENGINEERING

JOB SAFETY ANALYSIS			
JSA No.:	BL-SEM-01	**Activity Planned Date**	According to testing plan
ACTIVITY:	SHS COLUMN COMPRESSION TEST		
*Required Personal Protective Equipment (PPE) for entire Job		Hard hat, gloves, safety goggles, safety boots, laboratory coat	

Step No.	**Step activity**	**Potential Hazards**	**Hazard Mitigation Measures**
1	Transport specimens from workshop to testing area as well as other setup tools to testing area	- Objects falling - Sharp edges	- Take care and be cautious when - handling objects Wear the appropriate PPE
2	Mark out centre point of testing plates	- Contact with testing plates	- Wear hard boots, gloves and laboratory coat
3	Place specimen centre on machine base	- Contact with testing plates	- Wear hard boots, gloves and laboratory coat
4	Lower the platen until it just contacts top specimen plate	- Loading plates injuring fingers when lowered	- Make use of slow loading rate and control it so that machine is stopped gently at point of contact
5	Restrain the top fixed end plate to the loading late by threading a ratchet rope through the specimen hooks and tying securely to plate	- Rope not tightened adequately, and specimen pops out during testing.	- Ensure rope is taut. - Close the Perspex glass shield
6	Once specimen is secured run the compression test to failure	- Specimen pops out during testing due to unsecure rope and load application from the machine.	- Observe tautness of rope during testing Maintain a safe distance - from machine during testing - Secure the Perspex glass shields around specimen

JOB SAFETY ANALYSIS CONTINUED…			
Step No.	**Step activity**	**Potential Hazards**	**Hazard Mitigation Measures**
7	Remove load and unrestraint the failed specimen	Specimen falling	Exercise caution when removing specimens
8	Dispose of the failed specimen in a designated area	Objects falling Sharp edges	Take care and be cautious when handling objects Wear the appropriate PPE

By: Bijal Larknath…….. **Sign:BL.....Date: 9 November 2023**
Checked (Lab Manager/Supervisor): Kenny Mudenda Sign: KM .....Date:9 November 2023

Appendix F: GANT Chart

2023 GANT CHART														
TASK TYPE	TASK	MONTH	FEB	MAR	APR	MAY	JUN	JUL	AUG	SEP	OCT	NOV		DEC
WRITTEN	LIT REVIEW		23			2								
WRITTEN	PROPSAL (DRAFT 1)		23	23										
WRITTEN	PROPOSAL+LIT REVIEW (DRAFT 2)					12				11				
PRACTICAL	SPECIMEN DRAWING								4					
PRACTICAL	LAB INDUCTION						15							
PRACTICAL	MATERIAL ORDER							31						
PRACTICAL	MATERIAL RECEIVED								23					
PRACTICAL	MATERIAL GIVEN TO WORKSHOP								24					
PRACTICAL	FABRICATION									5		8		
PRACTICAL	TESTION HOLLOW SECTIONS										30-31			
PRACTICAL	TENSILE TESTING											8		
PRACTICAL	FEM										21	17		
WRITTEN	FINAL WRITE UP									15		20		